A critical review of arsenic occurrence, fate and transport in natural and modified groundwater systems in The Netherlands

Stuyfzand, Pieter J.; Bonte, Matthijs

Important note
To cite this publication, please use the final published version (if applicable).
Please check the document version above.

A critical review of arsenic occurrence, fate and transport in natural and modified groundwater systems in The Netherlands

Pieter J. Stuyfzand [a,b], Matthijs Bonte [c,*]

[a] Stuyfzand Hydroconsult+, Zandvoort, the Netherlands
[b] CEG, Technical University Delft, the Netherlands
[c] MB-Water, Amsterdam, the Netherlands

ARTICLE INFO

ABSTRACT

Arsenic is a common trace element in groundwater and its fate and transport are controlled by combination of (i) natural processes, including redox conditions, salinity and pH, (ii) sedimentary and geochemical environment, and (iii) anthropogenic influences such as groundwater extraction, managed aquifer recharge (MAR), Aquifer Thermal Energy Storage (ATES), and pollution. We investigated the relative influence of these processes by presenting 10 cases from The Netherlands. Our review showed that the primary controlling factor for arsenic mobility in natural coastal dune systems is the redox state of groundwater, with concentrations between 2 and 10 μg/L. Strongly reduced greensands (containing glauconite and, more importantly, associated minerals) exhibited elevated As concentrations, with concentrations up to 40 μg/L. Groundwater systems modified by MAR or those that are influenced by nitrate pollution (NP) showed elevated As concentrations (20–110 μg/L), as a result of either pyrite oxidation (MAR, NP) or reductive dissolution of iron(hydr)oxides (MAR). Increasing temperature at ATES systems may cause mobilization of As at temperatures beyond 25 °C. The highest As concentrations were observed at sites where muddy sediments were recently deposited in surface water bodies (200–820 μg/L), for example in dammed Rhine River tributaries and sand pit lakes south of the city of Amsterdam. The reduction of arsenate to arsenite and competitive desorption during intrusion of polluted water also form important As mobilizing processes. The data for the Netherlands show that high CH_4 and NH_4 concentrations may form a risk indicator of elevated As levels in some fresh groundwater systems.

1. Introduction

Arsenic (As) is a natural trace element commonly found in groundwater (Hem, 1985; Herath et al., 2016; Mattheβ, 1994; Ravenscroft et al., 2009; Smedley and Kinniburgh, 2002) with concentrations in many aquifers below drinking water standards (<10 μg/L). Elevated concentrations (up to several thousands of μg/L) are observed in specific environments, notably in thermal groundwater (Morales-Simfors and Bundschuh, 2022; Webster and Nordstrom, 2003; Welch et al., 2000; Xing et al., 2022), groundwater affected by mining activities (Coudert et al., 2020; Paktunc, 2013; Smedley et al., 1996; Williams et al., 1996), groundwater in tuffaceous rock (Johannesson and Tang, 2009), groundwater in closed basins with high evaporation rates (Dehbandi et al., 2019; Jia et al., 2017; Ortega-Guerrero, 2017; Smedley et al., 2002; Welch et al., 2000) and in deltas (Postma et al., 2007; Smedley, 2008; Smedley and Kinniburgh, 2002; Wang et al., 2018). Most

problematic are the deltas, like the ones in Bangladesh, West Bengal, Cambodia and Vietnam, because of widespread reliance on untreated groundwater as the main source of drinking water. The direct use of As containing groundwater for drinking water purposes results in elevated risk of skin disorders and various cancers (Bundschuh et al., 2005; Kapaj et al., 2006; Tchounwou et al., 2019; World Health Organization, 2019). Elevated As concentrations in groundwater are also reported in European countries including Belgium (Coetsiers and Walraevens, 2006; Vandenbohede et al., 2019) and Germany (Banning, 2021; Heinrichs and Udluft, 1999; Houben et al., 2017).

Areas with high As concentrations in groundwater combine several hydrogeochemical triggers to mobilize As, with a (past) hydrogeological regime to keep the As within the system (Smedley and Kinniburgh, 2002). The main triggers are: reductive desorption from and reductive dissolution of iron (hydr)oxides (like hydrous ferric oxides (HFO) and goethite), desorption and pyrite oxidation. A favorable (past)

---

hydrogeological regime consists of young fluvial, deltaic or estuarine sedimentary deposits rich in iron(hydr)oxides, pyrite and labile organic material, without previous extensive periods of leaching (Ravenscroft et al., 2009; Smedley and Kinniburgh, 2002).

These conditions are also abundantly present in the sediments that built the Quaternary deltas and fluvial plains in the Netherlands. Shallow water tables and the widespread occurrence of clay and peat layers resulted in predominantly reducing groundwater conditions. The situation changed roughly around 1000 AD when the inhabitants started cultivating the land which strongly impacted the hydrologic regime. This involved draining the land, building dikes for protection against marine and fluvial inundations, peat extraction and dewatering, reclaiming land from lakes and the sea, groundwater extraction and artificial recharge for water supply. Meanwhile groundwater levels are maintained within close boundaries by an intricate system of both draining and infiltration ditches and canals, regulated by weirs, sluices and pumps (Huisman et al., 1998; Mostert, 2020; Van de Ven, 2003). In addition, surface and groundwater pollution started on a large scale roughly since 1880 AD with a strong boost after World War 2, with major increases in salinity, NO_3, NH_4, SO_4, F, DOC, PO_4 and As. All these changes had and continue to have a profound impact on the spatial distribution of water types (Engelen, 1986; Stuyfzand, 1995).

Despite the presence of aquifers with abundant reactive components,

and a hydrogeological regime that has undergone severe changes and is under considerable pressure from polluting activities, the Netherlands have not been identified as a country with major As problems (Ahmad et al., 2020b; Brunt et al., 2004). This is probably because groundwater used for drinking water supply is treated by aeration and rapid sand filtration for iron removal which is very effective in removing As to <10 µg/L (Ahmad, 2020). Although there is a large body of literature on As occurrence in deltas in southeast Asia (Chakraborty et al., 2022; Hossain, 2006; Huq et al., 2020; Nickson et al., 1998; Pedersen et al., 2006), a reasonable number of studies in other regions like the United States (for example Welch et al., 2000), and research in Germany and Belgium (Banning, 2021; Coetsiers and Walraevens, 2006; Heinrichs and Udluft, 1999; Houben et al., 2017; Vandenbohede et al., 2019), relatively little is reported in literature on arsenic in the Netherlands (Ahmad et al., 2020b; Spijker, 2008; Vermooten and Gunnink, 2006; Stuyfzand et al., 2008). In order to fill this gap, this work presents an overview on arsenic occurrence in 10 groundwater flow systems in the Netherlands, including both natural and anthropogenically influenced systems. The focus is on revealing patterns as based on major-ion and trace-element data (without As speciation but with bulk geochemical data), with special attention to i) surface water – groundwater interaction (including the effects of muddy fine-grained sediments depositing in relatively stagnant areas of highly managed surface water systems), ii)
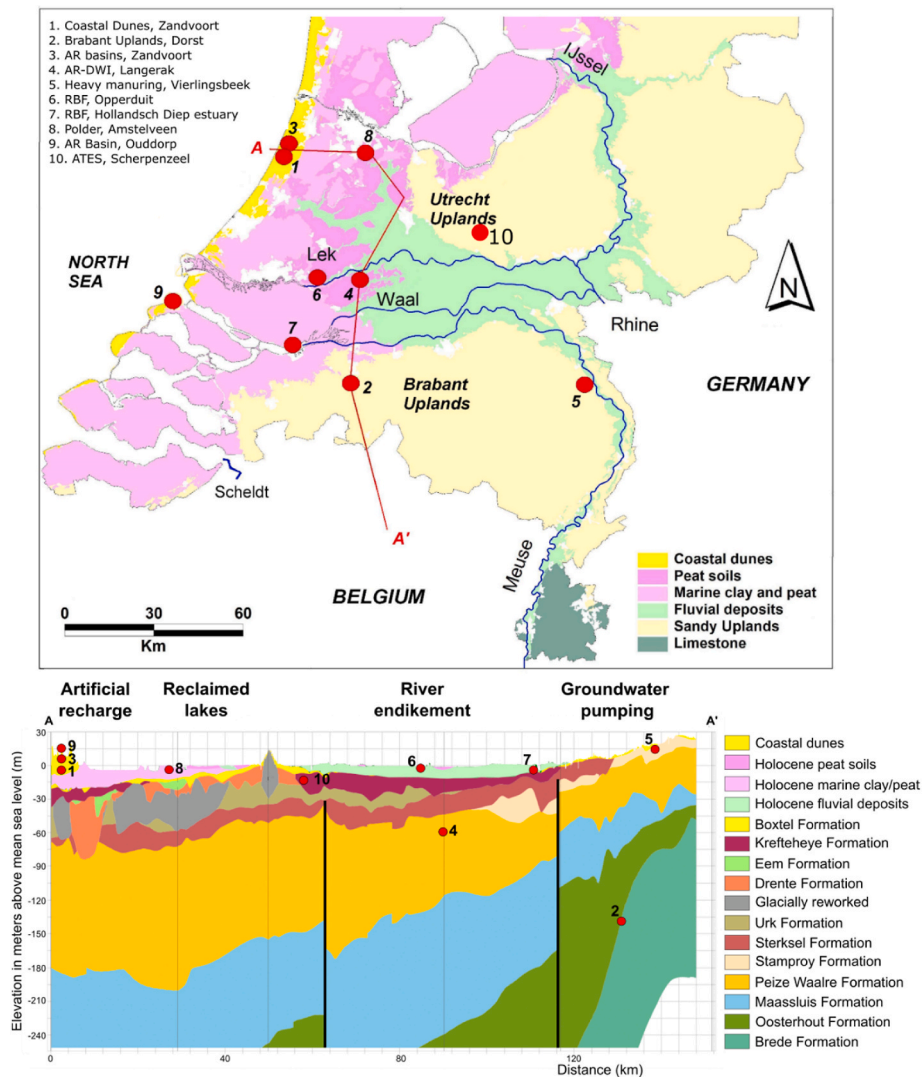

Fig. 1. Top panel: Landscape map of the Netherlands showing the 10 study sites and the position of cross section AA' (bottom panel). Bottom panel: Geological Cross section AA' over the Netherlands from the North Sea into Northern Belgium (Modified from TNO, n.d.).

artificial recharge systems, and iii) impacts of temperature perturbations in shallow geothermal energy systems (also known as aquifer thermal energy storage). The overview will help researchers and water managers to identify settings or activities that may mobilize and increase aqueous concentrations of arsenic.

2. Field sites and methods

2.1. Setting

The focus is on a selection of detailed hydrochemical and geochemical field studies that have been conducted on various sites in the Netherlands (Fig. 1, Table 1, Figure SI1). A cross section over the Netherlands (Fig. 1) shows the position of the study sites in their geological and hydrological setting, and how the spatial distribution of groundwater bodies probably changed during the past millennium.

2.2. Groundwater sampling

Groundwater samples were taken and analyzed from dedicated monitoring wells in the period 1980–2014, during various regional and local surveys (Table 1). The samples from sites 1–6 and 8–9 are derived from individual or nested PVC piezometers with a 0.2–2 m long well screen, or from a set of 10–30 PE miniscreens (0.01 m) attached to a 25–35 m deep piezometer. At site 7, samples were taken, both on land and from a boat, via a direct push, groundwater sampler mounted in a cone tip during cone penetration testing. The piezometers were installed in percussion drilled bore holes. At site 10, samples were taken during flow through column testing experiments in a laboratory setup (Bonte et al. 2013a).

Sample conservation for cations, SiO_2, PO_4 and trace elements including total As consisted of on-site filtration over 0.45 μm membrane filter, acidification by 65% HNO_3 suprapure (0.7 mL/100 mL), and storage in the dark at 4 °C. Samples for Cl, SO_4, HCO_3, NO_3, NH_4, F and DOC, for CH_4 and for ^{18}O–H_2O were taken without filtration and without additives for conservation, in 3 separate vials with an air-tight cap construction, and stored in the dark at 4 °C. Chemical analysis typically occurred within 0.5–7 days.

2.3. Sediment sampling

In total 908 sediment samples were taken on around 100 sites, from 0 to 300 m-LS depth. Various sampling and preservation methods were applied. Samples from the unsaturated zone were taken by either a hand auger or a direct push core sampler, and stored under atmospheric conditions at 4 °C in the dark.

Underwater muds and sediments up to 20 m below them were sampled via a direct push core sampling system. Aquifer and aquitard material from deep drillings for installation of monitoring wells (20-300 m-LS) were sampled through either core catchers ahead of the drilling casing, or directly from a bailer. Most sediment cores from core catchers including their pore water were immediately sealed on site using liquidized paraffin, and kept at 4 °C in the dark until analysis. Samples taken from a bailer or otherwise were stored under atmospheric conditions at 4 °C in the dark.

2.4. Hydrochemical analyses

Temperature, pH, SEC and O_2 were normally measured in the field. Major cations and anions, CH_4 and DOC were analyzed using conventional, well standardized techniques by certified laboratories. Samples with elevated CH_4 concentrations (roughly >15 mg/L) suffered from CH_4 losses by bubble formation and degassing during vacuum sampling. The resulting data are treated as underestimates. Total aqueous arsenic was analyzed in most cases through either AAS hydride with graphite furnace (limit of quantification [LOQ] 0.5–1 μg/L), or ICP-MS (LOQ 0.1–0.5 μg/L). The quality of analytical data of major ions was checked by the charge balance and by comparing the measured with calculated EC. Precision of the As measurements in groundwater was about ±(5–10)%, the accuracy had about the same range (evidenced by comparing groundwater samples with different methods and standard addition).

Naturally recharged (through rainfall) groundwater, artificially recharged surface water (AR) and river bank filtrate (RBF) were identified by using a combination of the environmental tracers $\delta^{18}O$ and the Cl/Br-ratio (Stuyfzand et al., 2005). Groundwater ages were estimated by comparison of tracer input concentrations (^3H, Cl) with their spatial distribution or tracer output record in groundwater, hydrological

Table 1

Summary of data regarding the 10 study sites. Site numbers correspond with location map in Fig. 1. AR = Artificial Recharge via basins; ATES = Aquifer Thermal Energy Storage; DWI = AR via Deep Well Injection. LS = Land Surface; RBF = River Bank Filtration; SL = Sea Level.

| Site | | Geological deposits flushed | Recharging water type | As-max | | | Sampling | Reference |
No.	Name			μg/L	Depth [m-LS]	Age [a]	year	
1	Zandvoort dunes	Holocene coastal dune and marine sands	Coastal rain	2–10[&]	9	10	2007	Stuyfzand (1993a, 1993b)
2	West-Brabant uplands (Dorst)	Pleistocene fluvial and marine sands/loams, Upper Tertiary glauconitic sands	Rainfall	25–40[$]	175	2000–10,000	2003	This paper
3	AR, Zandvoort	Holocene coastal dune and marine sands	Rhine River water (pre-treated)	50	13	4–20	2007	Stuyfzand (1993b, 2015)
4	DWI, Langerak	Pleistocene fluvial sands	Drinking water (injected)	90	92	0.02–0.5	1996–1998	Stuyfzand and Timmer (1999)
5	Vierlingsbeek	Pleistocene and Tertiary sands	Inland rain, fertilizer inputs	110	27	30–40	1988	Van Beek et al. (1989, 1988)
6	RBF Opperduit	Recent mud[@], Holocene and Pleistocene fluvial sands	Rhine River water (bank filtrate)	200	5–15	0.2–4	1983	Stuyfzand et al. (2006)
7	RBF Hollandsch Diep	Recent mud[@], marine Holocene and fluvial Pleistocene sands/clays	Rhine + Meuse River water (bank filtrate)	420	12–15	10–25	1997	Stuyfzand et al. (2005, 2006)
8	Polders south of Amsterdam	Recent mud[@], Holocene peat and marine clay, Pleistocene fluvial sands	Polder waters[#]	880	30	20–200	1996	Van Rossum (1998)
9	AR Ouddorp	Holocene coastal dune and marine sands	Rhine (70%) + Meuse (30%) River (AR)	27	2–4	0.3–5	2014	Stuyfzand et al. (2014)
10	Scherpenzeel ATES experiments	Pleistocene fluvial sands	Inland rain	138	−35	N/A	2012	Bonte et al. (2013a, 2013b)

Notes: #: a mixture of Rhine River water and groundwater exfiltrated in deep polders; &: 2 in calcareous dunes Zandvoort, 10 in decalcified dunes 40 km north of Zandvoort; $: 25 near Dorst, 40 in glauconitic sands without fertilizer inputs on site 5; @ = mud formed and still residing underwater; N/A: Age data not available.

calculation and – in >150 years old groundwater – by ^{14}C dating.

The redox state of each sample was determined on the basis of all redox sensitive main components of water, i.e. O_2, NO_3, SO_4, Fe, Mn, CH_4 and H_2S, following the scheme in Table 2. The redox clustering (oxic, suboxic and anoxic) in Table 2 is used here because of lack of sufficient data on O_2, CH_4 and H_2S. The distinction between an iron-reducing (sulfate-stable) and sulfate-reducing environment can be problematic when H_2S data are lacking and the original SO_4 concentration before potential sulfate-reduction (which is indicated as $(SO_4)_0$) cannot be estimated. In case of infiltrating surface waters (as in AR and RBF systems) the $(SO_4)_0$ concentration was estimated by the strong positive, linear regression between Cl (considered conservative) and SO_4 (dependent variable).

2.5. Sediment geochemical analyses

Samples from a (sub)oxic environment were air dried and subsequently sieved, homogenized and split. About 60% of the anoxic samples derived from cores were treated in a glove box under N_2 atmosphere and not dried, except for a fraction to determine its dry weight. The other 40% was treated without excluding air, which led to partial oxidation of reduced components such as pyrite. This did not affect the elemental composition of the samples, but excluded them from more detailed analysis (results not included in this paper). All samples were sieved over mesh 2 mm to remove the gravel size fraction. Gravel consisting of quartz or siliceous rock was excluded from further analysis. Clay aggregates, peat, roots and shell fragments were ground and returned to the sieved sample. Sieved samples (the fraction <2 mm plus ground material) were manually homogenized and split into identical subsamples for separate analysis.

Geochemical analyses included: 1) Thermo-gravimetric Analysis (TGA; Dean, 1974; Rabenhorst, 1988) for dry weight residue, loss on ignition, and total carbonate content. 2) grain size analysis of the fraction <2 mm (after treatment with HCl and H_2O_2 to remove cementing materials), by a FRITSCH Laser Particle Sizer A22. Clay and silt fractions were converted to the traditional grain size analysis with pipette and sieves, by the approach of Konert and Vandenberghe (1997). 3) total organic C, total N and total S by pyrolysis and infrared gas detection. After acid washing to remove inorganic carbon and subsequent pyrolysis, C, N and S were measured on a LECO analyzer. Total C was also measured without acid washing, for calculating total carbonates. 4) XRF (X-ray Fluorescence) to determine total element content (30 species). The X-ray spectroscopy was performed with a ARL8410 spectrometer with a Rh tube, with full matrix correction for major elements, and Compton scatter method for trace elements. Precision and accuracy for As measurements in solids were about ±(5–20)% depending on method and concentration level, with a likely underestimate when using XRF due to volatilization losses. In the Supplementary Information, details are given on how to convert total S in iron-bound S.

3. Results and discussion

3.1. Arsenic in mineral phases

Table 2 presents an overview of the geochemical characteristics. Arsenic is present in the Dutch sediments in the following forms (Huisman, 1998; Van Rossum, 1996): (a) sorbed, largely as arsenate or arsenite to mainly Fe(III), Mn(IV) and Al (hydr)oxides, clay minerals and organic material; (b) an impurity in minerals like iron (hydr)oxides, pyrite (FeS_2, replacing S), monosulfides, acid-volatile sulfides and apatite ($Ca_5(PO_4)_3[OH,F,Cl]$, replacing PO_4); and (c) an arsenic mineral phase like arsenopyrite (FeAsS) and orpiment (As_2S_3).

Iron (hydr)oxides and pyrite (or other iron sulfides) are the dominant arsenic containing minerals. The importance of iron sulfides is supported by a positive linear relationship between total S or FeS_2 and As in anoxic sediments, which improves when looking at specific sediment types or locations (figures in SI). In the relation As = a + b S–FeS_2, constant 'a' represents the average amount of As contained in other phases than FeS_2. Constant 'b' normally varies between 0.002 and 0.006 on a molar basis (mol/mol), which ideally equals the stoichiometric As content of pyrite. This range corresponds with other data in the Netherlands (Broers and Buijs, 1997; Huisman, 1998), Germany (Cremer et al., 2003) and Florida USA (Price and Pichler, 2006). Regression data revealed that the marine deposits show a higher non-pyrite bound As content than the fluvial deposits, while the As content of the pyrites is lower. Linear relations also hold for other important trace elements in pyrite, like Co, Ni and Zn (Figs. SI–3) but the relations for As are stronger than those for Co, Ni and Zn.

Glauconitic sands (marine sands with the Fe-clay mineral glauconite, commonly known as 'greensands') showed relatively high As concentrations (Table 2), and the highest not-pyrite bound contents of As, Co, Ni and Zn. Our bulk data are inconclusive as to whether this arsenic is associated with glauconite itself or high As contents of accessory minerals like phosphorite, apatite and carbonates (Flink, 1985). presented data on the composition of various glauconites of Upper Cretaceous age, showing As contents of 4–57 ppm.

The recent underwater muds and sludge in the Hollandsch Diep fresh water estuary (site 7) show very high As contents (Table 3) that are only partly linked to pyrite (Figs. SI–2). The remainder could be associated with arseniferous struvite ($NH_4MgPO_4.6H_2O$), a mineral that is normally formed in sewage treatment plants (Lin et al., 2016), but which is also observed in natural deposits (Donovan and Grimm, 2007) and which may incorporate significant amounts of As (Weil, 2008).

3.2. Arsenic occurrence and hydrochemical patterns at individual sites

Results of chemical analyses are shown in Table 4 for selected water samples taken at the 10 study sites, with indication of their approximate age and transport distance in the underground. It is assumed that, at the prevailing pH range of 4–8 in groundwater of the Netherlands, in (sub)

Table 2

Practical criteria for determining the redox environment of a water sample (modified after Stuyfzand, 1993b). Concentrations in mg/L.

Level	Un-mixed redox environment	Redox cluster	Criteria [mg/L]						
			O_2	NO_3^-	Mn^{2+}	Fe^{2+}	SO_4^{2-}	H_2S^a	CH_4
1	Oxic	Oxic	$O_2 \geq 0.8\ (O_2)_{SAT}$		<0.1	<0.1	$\geq 0.8\ (SO_4)_O$	no	<0.1
2	O2-reducing		$O_2 < 0.8\ (O_2)_{SAT}$		<0.1	<0.1	$\geq 0.8\ (SO_4)_O$	no	<0.1
3	NO_3-reducing	Suboxic	<1	≥ 1	<0.1	<0.1	$\geq 0.8\ (SO_4)_O$	no	<0.1
4	Mn-reducing		<1	<1	≥ 0.1	<0.1	$\geq 0.8\ (SO_4)_O$	no	<0.1
5	Iron reducing		<1	<1		≥ 0.1	$\geq 0.8\ (SO_4)_O$	no	<0.2
6	Sulfate reducing	Anoxic	<1	<1			0.2–0.8 (SO4)$_O$	yes	0.2–0.5
7	Methanogenic		<1	<1			<0.2 (SO4)$_O$		≥ 0.5

Notes.

$(O_2)_{SAT}$: calculated saturation with atmospheric O_2.

$(SO_4)_0$ = original SO_4 concentration [mg/L], see text.

[a] Yes/no = yes/no clear H_2S-smell in field, or $H_2S \geq$ /< 0.1 mg/L. If data unavailable not a criterion.

Table 3
Survey of the average geochemical composition of un-cemented Recent, Holocene, Pleistocene and Upper Tertiary sediments in the Netherlands. LS = Land Surface % = mass % (dry weight).

Age	Site No.	Lithological description	Sample Depth m-LS	Number Samples n	Grains <2 um %	Bulk Organic %	CaCO₃ %	S total ppm	FeS₂ Max ppm	XRF Al %	XRF Ca %	XRF Fe %
Recent	7	Underwater mud, Estuary	1.8	66	15.3	7.27	7.66	2444	3821	3.89	3.83	2.40
Holocene	1, 3, 9	Young dune sand	2.6	19	1.1	0.59	2.87	<50	0	1.88	2.33	0.55
Holocene	1, 9	Old dune sand	0.6	10	0.9	0.83	0.02	<10	0	1.52	0.14	0.27
Holocene	1	Dune peat (1A₂ in Fig. 3)	3.6	10		55.30	29.2	6920	7231	0.76	13.01	3.49
Holocene	1, 3, 9	Marine sands and clay	10.9	40	3.0	0.27	8.99	583	1063	2.01	4.78	0.67
Holocene	8, 9	Holland peat, polder	2.0	46	–	47.40	–	17300	27468	2.34	5.00	3.53
Holocene	8	Marine clay	5.0	98	–	15.00	–	5900	9488	5.20	5.81	3.44
Holocene	8	Basal peat	9.0	213	–	56.10	–	30100	50518	1.32	6.09	6.09
Pleistocene	1–4	Fluvial sands & loams	32.4	287	3.2	0.34	1.55	289	505	1.66	1.05	0.62
Pleistocene	2	Marine sands	54.4	45	2.0	0.29	6.34	528	957	1.13	2.09	0.61
Pleistocene	10	Fluvial sands	35.0	2	1.3	0.20	0.74	500	900	0.68	0.28	0.07
Tertiary	2	Marine sands/clay, +glau@	82.2	22	10.6	0.52	8.17	3342	6199	1.89	2.85	2.98
Tertiary	2	Fluvial sands	202.7	52	2.1	3.64	0.05	1376	2198	1.19	0.09	1.11

Age	Site No.	Lithological description	Sample Depth m-LS	XRF K %	Mg %	Mn %	Si %	P %	As ppm	Co ppm	Ni ppm	Zn ppm
Recent	7	Underwater mud, Estuary	1.8	1.50	0.67	0.07	31.90	0.267	35.3	–	44	781
Holocene	1, 3, 9	Young dune sand	2.6	1.07	0.08	0.01	40.88	0.018	1.0	1.2	8.7	11
Holocene	1, 9	Old dune sand	0.6	0.84	0.02	0.01	43.80	0.014	1.9	0.5	2.6	8
Holocene	1	Dune peat	3.6	0.47	0.10	0.12	7.96	0.110	12.5	–	–	–
Holocene	1, 3, 9	Marine sands and clay	10.9	1.11	0.20	0.01	37.14	0.021	3.8	1.1	8.8	12
Holocene	8, 9	Holland peat, polder	2.0	0.98	0.53	0.12	13.50	0.130	13.5	–	–	–
Holocene	8	Marine clay	5.0	1.78	0.93	0.09	26.40	0.080	14.1	–	–	–
Holocene	8	Basal peat	9.0	0.54	0.45	0.12	6.90	0.080	84.3	–	–	–
Pleistocene	1–4	Fluvial sands & loams	32.4	0.87	0.11	0.01	42.64	0.013	3.0	1.6	9.2	15
Pleistocene	2	Marine sands	54.4	0.68	0.10	0.01	41.92	0.021	2.7	2.5	7.9	14
Pleistocene	10	Fluvial sands	35.0	0.55	0.13	0.15	43.09	0.00	3.7	2.6	7.4	8
Tertiary	2	Marine sands/clay, +glau@	82.2	0.92	0.22	0.02	37.81	0.041	16.3	5.9	11.1	33
Tertiary	2	Fluvial sands	202.7	0.57	0.03	0.02	42.84	0.007	5.1	1.6	6.1	12

Note: @: glau = glauconite + associated minerals such as phosphorite and apatite.

oxic environment As(V) as $H_2AsO_4^-$ or $HAsO_4^{2-}$ is dominant, and under anoxic redox conditions As(III) as H_3AsO_3 (Smedley, 2008). This was confirmed by arsenic speciation calculations using PHREEQCv.2 with the Wateq4F database (Parkhurst and Appelo, 1999), and by Dutch data sets (Ahmad et al., 2015; Van Rossum, 1996, 1998). A further presentation and elaboration of the data follow in the following sections together with site specific background information.

3.2.1. Site 1: A relatively undisturbed coastal dune aquifer system (Zandvoort)

The hydrochemical evolution of dune groundwater is discussed along a flow path starting at the recharge area in the calcareous dunes to its exfiltration in the Haarlemmermeer polder (Table 4 and Fig. 2). Background details about this study are given by (Stuyfzand, 1993a, 1993b). Arsenic ranged between 0.3 and 1.5 μg/L near the infiltration zone, which likely results from atmospheric input (0.2 μg/L in rainfall which is evapoconcentrated to 0.3 μg/L) and reaches a maximum concentration of 2.1 μg/L in the anoxic marine sands of zone C. This is followed in zone D by a reduction of As concentrations that coincides with an increase in Fe and SO₄ concentration. The SO₄ increase relates to higher atmospheric inputs. The As behavior in zones BCD differs from the general pattern of As and Fe increasing together when the water is becoming anoxic. The anomalous As behavior (decreasing when Fe is increasing) is not understood. It could reflect the atmospheric input record of As.

Arsenic increases slightly down-gradient (zones E and F) but remains ≤1 μg/L. The abrupt SO₄ reduction in Holocene clay (zone E) is inferred to be the result of pyrite precipitation. Similar patterns were obtained in neighboring wells and other dune areas, including decalcified dunes, all showing maximum As concentrations up to 10 μg/L, a few meters below the groundwater table.

Geochemical analyses revealed a relatively high arsenic content in dune peat layer 1A₂ (Table 3), but arsenic concentrations directly below these shallow peat layers remain <2 μg/L (Fig. 3). Either the As was present in a form that is not leachable or it was sequestered quickly after being leached. The chemical data showed a reduction in SO₄ concentrations and increase in NH₄ for groundwater passing especially through peat layer 1A₃ indicating anaerobic mineralization of peat coupled to sulfate reduction. This likely resulted in the formation of sulfides which can sequester leached arsenic as demonstrated by X-ray absorption spectroscopy for a wetland in Switzerland by (Langner et al., 2012).

3.2.2. Site 2: A relatively undisturbed glauconitic aquifer system (Dorst, Brabant)

Well field Dorst in the south of the Netherlands extracts 5.8 Mm³/a from an anoxic, confined aquifer at 118-183 m-SL. This aquifer is composed of marine glauconitic sands belonging to the marine Pliocene Oosterhout and Miocene Breda Formations. Recharge of this northward dipping aquifer occurs in the Kempian hills of Northern Belgium (30–40 km to the south).

Contrary to most other sites where highest As concentrations were observed at shallow depth (<20m-SL), here the highest As concentrations of up to 25 μg/L were observed in the glauconitic sands below somewhere between 120 and 170 m-LS (Fig. 4). There are no indications of pyrite oxidation, the water is several thousands of years old (³H < 1 TU, ¹⁴C = 10–32 pmc), calcareous and anoxic (however with a low CH₄ concentration, which is remarkable). The relatively high Na, K and Mg concentrations compared to Cl (Table 4) suggests cation exchange of these species with Ca due to freshening of the formerly more saline aquifer (Stuyfzand, 1993a). Elevated As concentrations have been observed in many more monitoring wells in Miocene/Pliocene aquifers of the Southern Netherlands (Flink, 1985) and Northern Belgium

Table 4

Summary of hydrochemical data for the 10 study sites.

Sample No.	Code	Depth m + SL[1]	Subsoil flow [m]	age	pH –	T °C	Cl mg/L	SO₄	HCO₃	NO₃	PO₄	F	Na	K	Ca	Mg	Fe	Mn	NH₄	SiO₂	DOC	As µg/L	Co	Ni	Zn	O₂ mg/L	CH₄
SITE 1	SITE 1. COASTAL DUNES, ZANDVOORT																										
1	Rain 1991-99	4	0	0	5.80	10.0	23	7.4	2.6	3.90	0.05	24	13.1	0.7	1.6	1.7	0.13	0.014	0.93	0.3	1.7	0.7	<0.9	2.5	16.8	10.8	<0.01
2	24H470	−0.4	5	1.4y	7.84	16.2	33	7.8	192	10.88	0.08	150	21.8	4.3	63.9	4.9	0.01	0.029	<0.004	5.1	4.2	0.5	0.13	1.6	4.5	<1	<0.01
3	24H470	−4.9	15	7y	7.80	15.5	43	28.4	222	<0.1	0.23	90	26.7	3.0	78.2	6.0	0.22	0.052	0.007	6.4	1.4	2.1	0.01	0.1	3.0	<0.1	<0.01
4	24H470	−13.6	33	20y	7.78	13.6	84	44.6	208	<0.1	0.71	90	44.0	1.9	88.8	5.3	1.86	0.29	0.50	23.6	1.3	<0.5	0.01	0.1	2.1	<0.1	<0.1
5	24H379	−21	28	25y	7.30	10.0	31	12.0	325	<0.1	1.32	40	19	1.8	103	4.2	6.87	0.50	1.70	32.6	–	0.3	<0.1	0.6	<5	<0.2	–
6	24H536	−57	1000	120y	7.30	10.8	41	<0.1	312	<0.1	1.4	60	22	4.4	90	6.2	2.30	0.42	2.80	30.8	6.0	1.0	<0.05	<0.5	<10	<0.2	–
7	24H450	−77	3500	400y	7.20	11.3	33	<0.1	365	<0.1	2.6	70	43	19.8	20.6	2.31	0.22	1.50	18.6	6.5	1.2	<0.05	<0.5	9	<0.2	–
8	24H600	−69	5500	600y	7.30	11.4	68	<0.1	540	<0.1	4.07	100	97	27.6	45	44.5	1.61	0.10	4.60	14.7	10.8	1.0	<0.05	<0.5	<10	<0.2	–
9	25C291	−60	7000	800y	7.30	11.6	225	6.0	927	<0.1	5.1	300	400	40	34	13.8	1.80	0.03	4.60	26.0	70	1.0	<0.05	<0.5	<10	<0.2	–
	SITE 2. GLAUCONIFEROUS SANDS, DORST (BRABANT)																										
10	49F235 no glau	−50	500	>100y	5.6	–	11	11.0	16	<0.1	1.22	80	8.0	1.5	4.3	0.8	2.45	0.03	–	16.9	–	1.1	<4	<6.5	23	<0.1	<0.1
11	49F235 no glau	−104	3000	>200y	7.8	–	8	3.0	204	<0.1	0.77	140	6.7	1.3	60	2.2	2.50	0.25	–	24.0	–	1.5	<4	<6.5	47	<0.1	<0.1
12	49F235 + glau[2]	−151	30,000	>2,000y	7.7	–	25	1.0	447	<0.1	1.68	360	96.0	22.4	45	14.8	1.10	0.93	–	16.9	–	22.0	<0.4	<6.5	16	<0.1	<0.1
13	50E377 + glau[2]	−163	33,000	>3,000y	7.62	18.1	9	0.2	195	<0.1	–	–	14.0	19.0	38	18.0	0.77	0.02	0.55	–	1.9	25.0	1.0	–	–	<0.1	0.05
14	50B340 + glau[2]	−189	35,000	>3,000y	7.77	13.4	16	1.9	270	<0.1	–	–	23.0	18.0	33	20.0	0.84	0.34	0.85	–	2.6	24.0	2.0	–	–	<0.1	0.35
15	50E377 + glau[2]	−208	37,000	>3,000y	7.83	18.5	11	<0.1	260	<0.1	–	–	13.0	18.0	38	17.0	0.71	0.02	1.10	–	2.1	25.0	0.0	–	–	<0.1	0.16
	SITE 3. ARTIFICIAL RECHARGE (BASINS), ZANDVOORT																										
16	Input 2006	0	0	0	7.80	12.9	100	60.2	157	11.4	0.02	110	48.6	4.6	76.0	10.4	0.01	0	0.01	5.0	2.5	0.2	0.19	1.6	2.4	9.3	<0.01
17	24H478	1.6	100	3y	7.46	13.9	100	67.6	167	16.2	0.08	200	45.0	5.4	84.5	11.1	0.01	0.001	0.001	5.0	1.6	<0.5	0.05	1.3	4.4	<1	<0.01
18	24H480	−9.4	350	12y	7.58	15.9	116	54.3	232	<0.1	0.12	70	74.1	2.0	96.4	3.3	4.28	1.10	0.54	15.7	3.3	33.2	0.42	0.3	5.3	<0.1	<0.1
19	24H480	−13.8	360	16y	7.76	16.4	144	39.3	253	<0.1	0.38	70	84.8	2.4	99.0	3.8	3.19	0.60	0.61	22.2	2.7	0.8	0.01	0.1	1.7	<0.1	<0.5
20	24H484	−18.6	810	26y	7.68	13.9	156	65.7	234	<0.1	1.04	110	33.3	3.3	160	7.8	0.58	1.14	1.56	58.4	2.9	3.1	0.01	0.1	1.2	<0.1	<0.5
	SITE 4. DEEP WELL INJECTION, LANGERAK																										
21	Input 1997	0	0	0	7.70	12.6	34	7.6	298	14.9	–	–	45.9	6.5	60.2	11.0	0.04	0.01	0.02	–	3.0	0.8	–	1.1	4	9.5	<0.01
22	W1-f3, 0 PFs	−91	20	6.4d	7.3	14.2	7	1.4	476	<0.1	–	–	73.5	5.3	69.4	11.1	2.31	0.14	1.17	–	5.2	0.5	–	1.0	10	<0.1	8.95
23	W1-f3, 2 PFs	−91	20	6.4d	7.4	12.7	88	19.5	286	1.3	–	–	79.0	5.5	62.8	9.7	1.57	0.10	1.11	–	3.4	90.0	–	0.5	5	0.5	0.43
24	W1-f3, 9 PFs	−91	20	6.4d	7.4	12.8	11	33.8	278	<0.1	–	–	37.8	5.8	61.7	10.2	1.63	0.10	0.21	–	2.3	4.0	–	0.5	5	<0.1	<0.01
25	W1-f3, 75 PFs	−91	20	6.4d	7.4	11.1	12	29.9	296	3.2	–	–	39.0	6.4	63.0	11.0	0.57	0.24	0.04	–	2.2	1.0	–	9.5	<5	0.7	0.02
	SITE 5. HIGH AGRICULTURAL INPUTS, VIERLINGSBEEK																										
26	46DNP3	14.8	300	6y	4.7	–	37	75.0	3	281	0.04	40	17.5	22.3	104	13.0	0.04	1.80	0.03	21.5	3.4	0.5	3.2	78.0	160.0	<1	<0.01
27	46DNP1	6.8	800	16y	6.1	–	47	96.0	125	85.3	0.04	40	33.0	38.0	70	14.3	0.03	0.44	3.90	10.0	9.1	1.0	135.0	465.0	150.0	<1	<0.01
28	46DNP1	−3.2	1200	24y	5.1	–	35	190.0	9	<0.1	0.05	–	15.0	8.0	52	16.0	5.5	0.31	0.08	13.0	1.7	75.0	25.0	100.0	10.0	<0.1	<0.1
29	46DNP1	−4.2	1300	26y	5.3	–	33	143.0	10	<0.1	0.05	–	13.5	6.0	40	12.3	7.5	0.29	0.09	13.5	1.3	110	29.0	125.0	5.0	<0.1	
30	46DNP1 +glau[2]	−22.2	2600	>50y	7.2	–	9	8.0	130	<0.1	4.30	–	5.5	1.4	37	2.3	8.8	0.50	0.32	18.5	0.9	40.0	5.6	2.0	10.0	<0.1	
	SITE 6. RIVER BANK FILTRATION, OPPERDUIT																										
31	Rhine 1983	0	0	0	7.8	12.8	141	67.0	161	15.9	1.00	210	78	6.1	74	10.6	0.59	0.08	0.53	5.6	4.6	1.1	0.6	4.6	26.0	8.8	<0.01
32	38D290-mf7	−10	20	<1y	7.10	–	171	6.0	686	<0.1	4.53	–	91	9.0	150	12.5	26.0	1.70	51.0	13.8	6.5	200	1.0	2.0	10.0	<0.1	–
33	38D292-mf4	−22	150	2.5y	7.5	–	148	70.0	188	<0.1	0.34	–	93	5.1	68	10.0	1.9	–	1.06	3.6	2.7	1.5	1.5	1.0	5.0	<0.1	0.12
34	38D294-mf7	−22	650	8y	7.5	–	137	52.0	226	<0.1	0.46	–	72	5.0	81	12.0	2.3	–	2.00	5.0	3.3	1.0	<0.5	<1	5.0	<0.1	0.13
	SITE 7. RIVER BANK FILTRATION, HOLLANDSCH DIEP ESTUARY																										
35	Input 1996	0	0	0	8.20	10.5	146	65.0	162	16.1	0.31	210	81	6.4	75	12.9	<0.2	<0.1	0.19	4.7	2.9	<2	–	3.4	–	9.2	<0.01
36	6-6 (type A)	−5.9	8	<5y	7.5	10.5	110	18.0	265	<0.1	5.51	270	59	6.3	88	11.0	2.0	0.60	3.0	27.0	6.0	6	–	2	56	<0.1	0.1
37	9-9 (type C)	−9.4	12	10y	6.80	10.5	260	<1	2400	<0.1	0.46	320	200	36.0	230	110.0	36.0	0.50	230	15.0	33.0	81	–	3	7	<0.1	>19.0
38	4-14 (type B)	−13.8	22	12y	7	10.5	130	<1	1120	<0.1	0.49	120	94	19.0	190	40.0	39.0	3.00	53.0	18.0	23.0	413	–	<1	<5	<0.1	>16.0
39	71-13 (type A)	−12.5	750	38y	6.9	10.5	290	<1	649	<0.1	0.37	260	160	7.2	160	25.0	15.0	1.90	5.4	22.0	11.0	0.4	–	<1	16	<0.1	16.0
40	1-22 (type F)	−22.2	800	75y	7	10.5	330	<1	650	<0.1	0.21	230	220	10.0	87	59.0	4.0	0.20	15.0	24.0	9.0	0.6	–	<1	7	<0.1	20.0
41	71-28 (type G)	−27.1	1400	125y	6.8	10.5	210	<1	451	<0.1	0.58	260	130	7.4	99	17.0	4.0	0.15	16.4	26.0	17.0	0.2	–	<1	13	<0.1	18.0
	SITE 8. POLDER SYSTEM, SOUTH OF AMSTERDAM																										
42	25GS001	−14.0	–	<300y	6.67	–	171	2	924	<0.1	9.14	–	128	28.6	126	68	9.2	0.83	39.5	24.9	–	141	–	–	–	<0.1	–
43	25G376	−19.5	–	<300y	6.95	–	189	1	1146	<0.1	–	–	201	31.4	76	97	12.2	0.05	16.6	19.8	–	216	–	–	–	<0.1	–
44	25GS001	−25.3	–	<300y	6.91	–	118	2	875	<0.1	6.57	–	152	25.0	85	56	13.2	0.18	20.0	16.4	–	404	–	–	–	<0.1	–

Table 4 (*continued*)

Sample No.	Code	Depth m + SL[1]	Subsoil flow [m]	age	pH	T °C	Cl	SO4	HCO3	NO3	PO4	F	Na	K	Ca	Mg	Fe	Mn	NH4	SiO2	DOC	As	Co	Ni	Zn	O2	CH4
		m + SL	flow [m]	age	–	°C	mg/L						mg/L									µg/L				mg/L	
45	25D1185	−27.0	–	<300y	7.53	–	222	3	762	<0.1	3.41	–	108	25.9	67	97	11.0	0.90	11.2	15.0	–	823	–	–	–	<0.1	–
46	25G376	−50.5	–	<300y	7.38	–	1338	9	1192	<0.1	–	–	1038	12.4	75	43	3.1	<0.02	3.1	13.6	–	26.9	–	–	–	<0.1	–
47	25G376	−82.5	–	–	7.23	–	3224	78	1124	<0.1	–	–	1829	33.7	178	127	2.7	0.62	6.2	10.8	–	4.0	–	–	–	<0.1	–
48	25G376	−149.5	–	6000	6.97	–	6385	553	467	<0.1	–	–	3306	85.4	363	352	7.3	0.14	6.1	11.6	–	1.0	–	–	–	<0.1	–
SITE 9. ARTIFICIAL RECHARGE (BASINS), OUDDORP																											
49	Input 2005-10	0	0	0	8	–	78	54	161	11.4	0.06	–	42	4.9	67	11	0.04	0.04	0.11	4.2	2.4	0.5	0.2	0.6	5.1	10.6	<0.01
50	Output 2005-10	−4	90	67 d	7.4	–	93.9	45.1	214	2.8	0.2	–	47.3	4.4	77.6	10.8	0.24	0.11	0.37	6.4	2.9	12	0.4	0.3	6	1.8	–
51	10.664-2	2.2	33	40 d	7.6	–	110	40	264	0.1	0.39	–	63	6.4	79	11	2.7	0.03	0.3	6.58	2.8	27.3	0.04	0.4	0.6	<0.5	0.49
SITE 10. COLUMN TESTING OF IMPACTS OF AQUIFER THERMAL ENERGY STORAGE AT SCHERPENZEEL																											
52	In-situ	−35	N/A	N/A	7.3	–	7.1	6	122	<0.25	0.2	64	5.6	0.8	29.9	2.2	0.3	0.08	0.09	5.2	0.6	6	1.4	8	30	<0.1	–
53	Max As @5 °C		4.2 PV	N/A	7.4	–	7.4	–	145	<0.25	0.08	70	6.2	1.1	36.6	2.8	0.36	0.06	0.06	6.1	0.8	11	0.7	5	1	<0.1	–
54	Max As @11 °C	N/A	0.9 PV	N/A	7.6	–	7.9	–	139	<0.25	1	90	7	1.5	36.9	2.8	0.3	0.06	0.02	6.1	1.9	16.5	1.4	1	11	<0.1	–
55	Max As @25 °C	N/A	3.6 PV	N/A	7.4	–	7.1	7.1	130	<0.25	0.08	110	6.4	2.7	38.7	3	0.4	0.07	0.02	7.3	2.1	33	1	1	1	<0.1	–
56	Max As @60 °C	N/A	2.2 PV	N/A	7.1	–	7.8	–	145	<0.25	0.4	##	8.5	2.1	42.2	3.1	0.4	0.08	0.04	13.6	4.8	138	<1	2.5	3	<0.1	–

Notes: + Glau = sand containing glauconite. SL = Sea Level.

(Coetsiers, 2007), also remote from well fields.

3.2.3. Site 3: Artificial recharge in coastal dunes (Zandvoort)

Since 1957, around 60 Mm^3/a of pretreated Rhine water recharges a large dune area south of the town of Zandvoort. The original infiltrated Rhine water is oxic (with Dissolved Oxygen, DO > 9 mg/L), followed by the subsequent consumption of DO and NO_3 during oxidation of sedimentary organic matter, inferred to represent a transition in redox zones from oxic to nitrate to iron reducing conditions (Table 4, Fig. 5). The position of the next redox boundary separating iron and sulfate reducing conditions (inferred from a reduction in sulfate concentrations) coincided more or less with the deeper parts of aquitard A. The ambient dune water is characterized by the absence of SO_4 and underlies the infiltrated Rhine water.

A distinct zone of high As concentrations was observed between 0 and 15 m below mean sea level in the anoxic parts of the Holocene beach and marine sands (Fig. 6). The upper part of this high As zone coincided with the change from aeolian to marine deposits and with the transition from nitrate to iron-reducing conditions. The subsequent reduction of As concentration with depth, coincided with the transition from iron reducing to sulfate reducing conditions (indicated by reducing sulfate concentrations). The coincident reduction in Fe and As suggests that produced sulfide likely precipitated as arseniferous pyrite.

This situation resembles the situation in the dunes without artificial recharge (site 1) but with higher As concentrations. This difference may be explained by differences in lithology and geochemistry, history and hydrochemical composition. The Holocene sediments found at site 3 contained more discontinuous dune peat layers and aquitard A has a finer texture. Geochemical analyses showed that peat and fine grained sediments have relatively high As concentrations. Another difference is the higher rate of historic groundwater extraction in the period 1853–1957 that occurred at site 3 resulting in groundwater drawdown of 4 m, compared to only 1 m at Site 1. Following the start of the artificial recharge, groundwater recovered and rose by 1–4 m at Site 3.

3.2.4. Site 4: Artificial recharge using deep well injection (Langerak)

Close to the town of Langerak, a deep well injection pilot was run for 20 months, recharging a semiconfined, anoxic, sandy aquifer with oxic drinking water (Table 4, Fig. 7). Further details on the pilot study are given by (Stuyfzand and Timmer, 1999) and (Saaltink et al., 2003). Mass balances revealed that both O_2 and NO_3 oxidized pyrite, that contained significant amounts of As, Co, Ni and Zn (Table 3 and SI). This resulted in a front of mobilized As close to the injection well, which was largely immobilized further down gradient by adsorption to, or co-precipitation with, neo-formed iron(hydr)oxides (Fig. 8). Arsenic leaching declined substantially after flushing of the aquifer matrix with 10 pore volumes of infiltrated water (PVs), while elevated SO_4 concentrations in the observation well at 20 m distance suggested ongoing pyrite oxidation during the entire pilot (>88 PVs). This is explained by the initial lack of (a) complete oxidation of the mobilized As (probably as H_3AsO_3) to AsO_4^{3-} and (b) sufficient sorption sites on neo-forming iron (hydr)oxides. Also Ni mobilized from pyrite, but showed a significant delay in the calcareous aquifer with respect to As (Fig. 8, Table 4). The highest As concentrations were observed at 1.6 PVs, whilst for Ni highest concentrations were observed around 75 PVs.

3.2.5. Site 5: An aquifer system with strong nitrate pollution (Vierlingsbeek)

A phreatic well field near the town of Vierlingsbeek extracted 3–5 Mm^3/a of groundwater for around half a century starting since 1965. Land use in the catchment area was dominated by agriculture with high fertilizers use. The high input of nitrate resulted in extensive oxidation of pyrite in the sediment below 1–6 m + SL, which led to elevated SO_4 and As levels in extracted groundwater (Smolders et al., 2010; Van Beek et al., 1989, 1988; Van Beek and Van der Jagt, 1996). Pyrite facilitated denitrification is widely reported in sandy aquifers which are impacted by excessive fertilization (Jessen et al., 2017; Zhang et al., 2009, 2012).
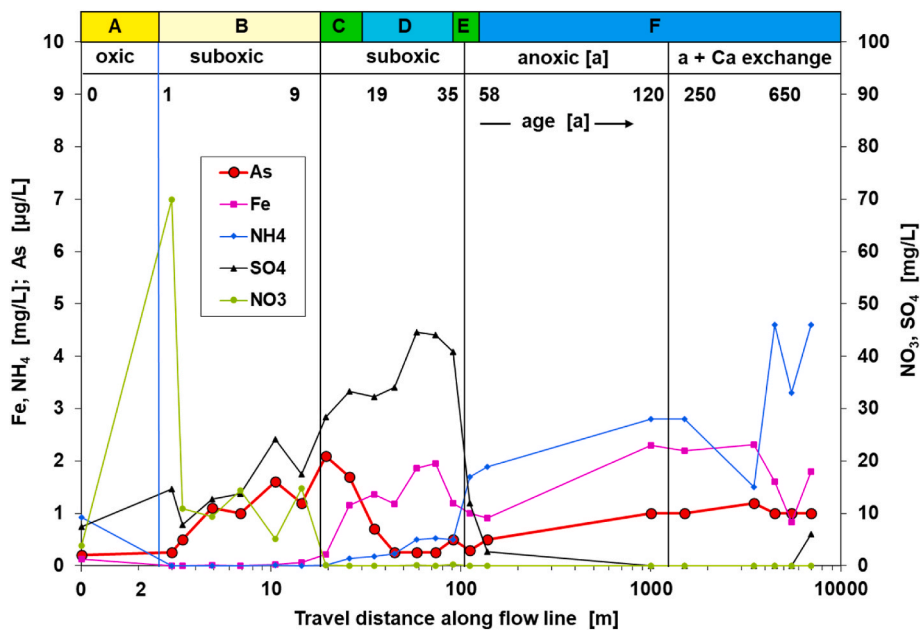
Fig. 2. Site 1: Concentration patterns of total As and redox sensitive major ions in coastal dune groundwater along a flow-path from infiltration area (calcareous dunes) to exfiltration area in the reclaimed lake Haarlemmermeer. Redox zones and approximate groundwater age are indicated at top. a = anoxic; A = Holocene dune sand in unsaturated zone; B = Holocene dune, beach and shallow marine sand; C = Holocene, marine, silty, very fine sand; D = Holocene marine sand; E = Holocene clay; F = Pleistocene deposits.
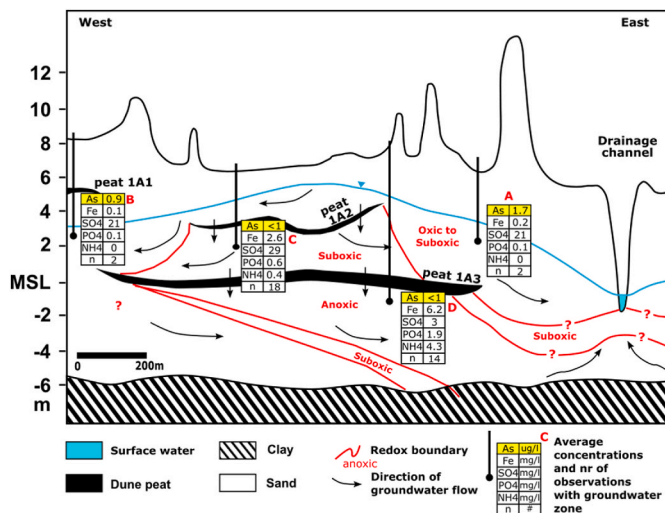

Fig. 3. Site 1: Mean composition of shallow dune groundwater as a function of dune peat interaction: $1A_1$ = thin peat layer permanently in unsaturated zone; $1A_2$ = thin peat layer permanently in saturated zone; $1A_3$ = relatively thick peat layer permanently in saturated zone. Pure dune peat groundwater = dune groundwater that passed the peat layer without mixing with dune groundwater that did not.

A–D = dissolved ions in groundwater for situation without peat (A; oxic to suboxic), with peat $1A_1$ (B; oxic to suboxic), with peat $1A_2$ (C; suboxic), and with peat $1A_3$ (D; anoxic). n = number of samples in area (Figure modified from Stuyfzand, 1993a; 1993b).

Fig. 4. Site 2: Arsenic and sulfate depth profile at the Dorst well field. The profile is based on average concentrations from 8 wells within a radius of 2 km around well field Dorst.

The spatial distribution of groundwater types showed that agricultural impacts were limited to the upper 20–25 m (Fig. 9, showing data for 1988). This resulted in (sub)oxic CaNO3 water (NO3 up to 330 mg/L) in the Pleistocene coarse sand and gravel aquifer, and an anoxic CaSO4 water type in the underlying, finer grained Pliocene sands. The highest concentrations are observed in NP.1 where SO4 and As reached 250 mg/L and 110 μg/L, respectively. The elevated As coincides with increasing concentrations of Co, Ni and Zn (Table 3). Ni concentrations were elevated over a larger depth zone than As (Fig. 13) which may be due to the low pH (4.5–6) resulting in differences in sorption between Ni and As. In addition, As is largely immobilized in the upper pyrite oxidation

zone by co-precipitation with neo-forming iron (hydr)oxides. Although groundwater below 10 m-SL is less influenced by nitrate pollution, As concentrations are still elevated (20–40 μg/L; Fig. 10). The absence of elevated Ni and Zn concentrations (which would derive from pyrite oxidation), overall natural groundwater composition (CaHCO3 type) and presence of glauconite in the Miocene deposits (as on site 2) suggests that the elevated As is of purely geogenic origin (deriving from minerals associated with greensand).

3.2.6. Site 6: Anoxic, Rhine River bank filtrate (Opperduit)

A former floodplain of the Lek river (a Rhine tributary) north of the town of Opperduit was embanked and drained in the 18th century, resulting in a so called polder. Continued drainage induced land subsidence, which in turn resulted in a hydrological setting where water from the river Lek infiltrates towards the aquifer and flows towards the floodplain. In 1983 and 1995 a transect of wells equipped with nested
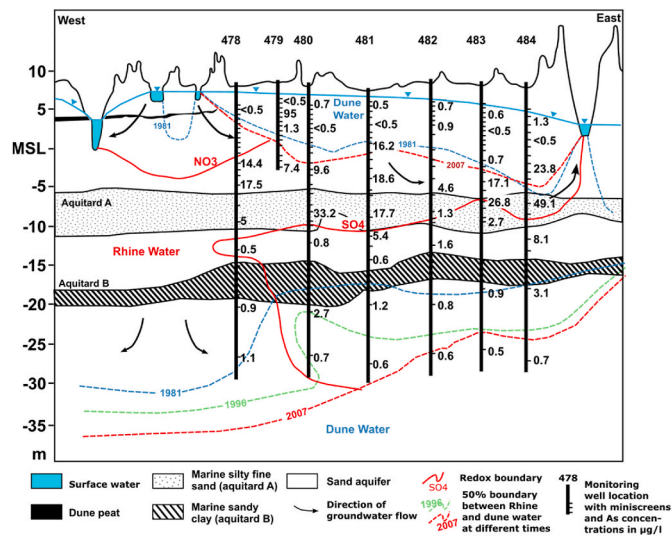
Fig. 5. Site 3: Distribution of groundwater bodies and As concentration (µg/L) in 7 multilevel monitoring wells in 2007. Well screen length < 0.5 cm (open end of small tube filled with glass wool). Rhine River water is recharging the dune sand aquifer via a supply canal and basins (modified after (Stuyfzand, 1993b)). A = moderate aquitard (c = 200 d); B = aquitard (c = 5000 d). Redox boundaries in Rhine infiltrate only: NO$_3$ = (sub)oxic; SO$_4$ = anoxic.

piezometers was sampled for extensive chemical analysis (Stuyfzand et al., 2006). Nearly all samples collected were anoxic. A plume of groundwater with elevated As concentrations (up to 200 µg/l) stretches from below the floodplain towards the former floodplain (Fig. 11). The elevated As is attributed by Stuyfzand et al. (2006) to the recent fluvial mud/sludge layer, deposited between the river groins, which likely acts as a substantial source of As, solutes like DOC, H$_2$S and CH$_4$, which may reduce iron (hydr)oxides and arsenate, and ions like PO$_4$, HCO$_3$, H$_4$SiO$_4$ and DOC which may compete with As for sorption sites on reactive minerals. The Opperduit case is representative for situations with sedimentation of underwater muds and sludge, with a high content of reactive young organic matter (for instance in gravel pits, harbors and closed meanders), which results in anoxic conditions.

3.2.7. Site 7: Anoxic, river bank filtrate in the Hollandsch Diep estuary

The Hollandsch Diep is part of the estuary formed by the Rhine and Meuse rivers. The flood protection of the Deltaworks (Dutch: Deltawerken), led to changing river flow conditions which resulted in the deposition of a 0.2–4 m thick mud layer on top of the sandy river bed at the northern part of the estuary (Fig. 12). The presence of a permanently drained deep polder north of the Hollandsch Diep (surface at 1.6 m-SL), resulted in continuous infiltration of the estuarine fresh surface water towards the aquifer, since the 17th century, which resulted in an intricate spatial pattern of groundwater quality as shown in Fig. 13 (Stuyfzand et al., 2004, 2006). Groundwater is anoxic with high CH$_4$ concentrations (up to 20 mg/l) especially in types B, C, F and G (Table 4). Groundwater types B and C have been in close contact with the recent mud layer, and are quite exceptional in their chemical composition with relatively high concentrations of As and other species including Ca, HCO$_3$, DOC, CH$_4$, NH$_4$, Mg, K, and Fe. This is thought to be the result of oxidation and fermentation of labile organic matter present in the mud, and As may have been derived from reducing iron (hydr) oxides in and below the mud layer. In addition, the mud layer is suspected to contain dissolving arseniferous struvite.

3.2.8. Site 8: polders south of Amsterdam

Several deep polders (4-6 m-SL) south of Amsterdam were reclaimed from lakes between 1700 and 1852 AD. These intensively drained severely polders impacted groundwater flow (Fig. 13) resulting in a flow direction from the surrounding peat lands and the surface water network. In these deep polders (Van Rossum, 1998) observed high As concentrations in the upper 50 m of groundwater (Fig. 13 and Table 4). High As contents were observed in the deepest of several peat layers (84 ppm; Table 3), while the highest As concentrations (100–823 µg/L) are associated with anoxic groundwater in the Pleistocene aquifer, and coincide with elevated concentrations of Fe, HCO$_3$, PO$_4$, and NH$_4$ (Table 4). This water is mostly fresh (Cl < 300 mg/L) and relatively young (<100 years, tritium often present), and infiltrated through discontinuities in the Holocene clay and peat aquitard. These discontinuities are formed by sandy infills of tidal gullies and rivers, relatively shallow peat excavations and canals (down to 5 m-SL) and deep sand pits (e.g. the Ouderkerkerplas extending to 45 m-SL). The As mobilization in the area may have multiple causes (Van Rossum, 1996, 1998): (i) local pyrite oxidation may have occurred at shallow depths near drainage systems and at depth within the Pleistocene aquifer; (ii)
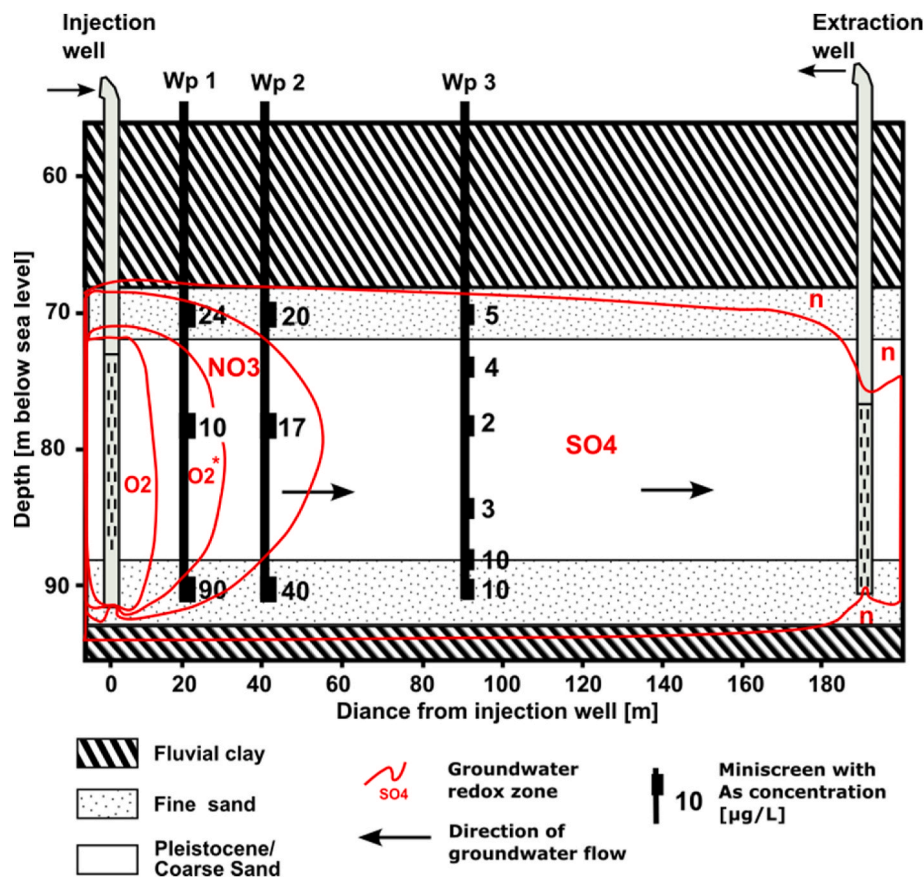

Fig. 6. Site 3: Arsenic profiles in groundwater in 2007 with the average hydrogeological bore log. The position of the mini-screened (with a screen length of <0.5 cm (open end of small tube filled with glass wool) monitoring wells 478–484 and the 3 groundwater types (shallow dune groundwater, Rhine infiltrate and deep dune groundwater) are indicated in Fig. 5.

Fig. 7. Site 4: Redox zonation in an originally anoxic aquifer after 1.5 years of deep well injection of oxic drinking water and distant recovery, and the As peak levels after ca. 2 pore volumes (modified from Stuyfzand and Timmer, 1999). O_2 = oxic (>90% O_2 saturated); O_2^* = soxic (<90% O_2 saturated); NO_3 = suboxic ($O_2 < 1$ mg/L, $NO_3 > 1$ mg/L), SO_4^* = anoxic ($O_2 = NO_3 = 0$, SO_4 above input due to pyrite oxidation); n = native, anoxic.
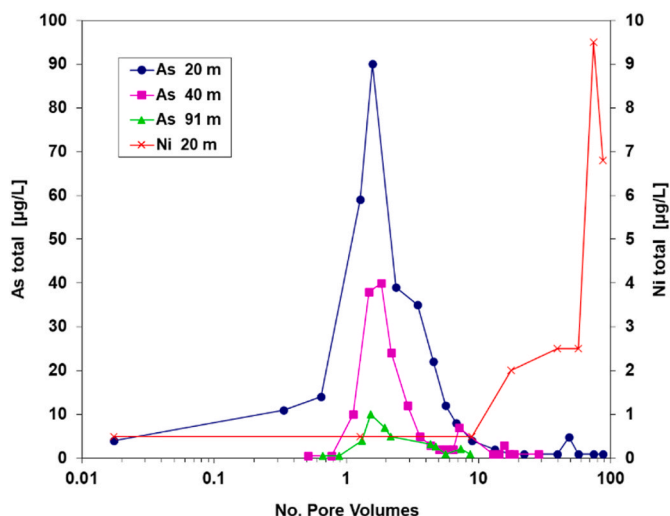

Fig. 8. Site 4: As and Ni mobilization in observation wells WP1-3 at ca. 90 m-LS (aquifer layer C) as a function of the number of pore flushes. Ni remained <1 μg/L at 40 and 91 m. Position of wells indicated in Fig. 7.

reductive dissolution of iron (hydr)oxides in the Holocene sediments and underlying Pleistocene sediments in combination with the reduction of As(V) to As(III); (iii) desorption of As(V) through raised concentrations of PO_4, H_4SiO_4, HCO_3, SO_4 and DOC in the infiltrating polluted surface waters that are composed of a mixture of Rhine River water and groundwater seepage from deep polders; and (iv) by ripening of iron

(hydr)oxides to more crystalline iron-minerals (e.g. goethite) which have less sorption sites.

3.2.9. Site 9: Arsenic problems due to ecological optimization of basin recharge system Ouddorp

At public supply well field Ouddorp (Fig. 1), AR has been applied as of 1955. The infiltration water was composed of untreated polder water (1955–1972), an untreated mixture of polder and fresh water from the Haringvliet lake (1972–1993), untreated Haringvliet water (1993–1995), and pre-treated Haringvliet water (1995-today). In 2007 an alarming rise of As concentrations was noticed in the raw water, which is still on-going. The level increased from ~3 μg/L in the year 2000 to ~13 μg/L in 2013, with a simultaneous increase in Fe, Mn, NH_4 and PO_4 concentrations (Fig. 14). A very similar As peak concentration had shown up already in 1983, also together with high Fe, Mn, NH_4 and PO_4 concentrations (Fig. 14). The As increase in the period 2000–2013 could be linked to ecological renovation works in 2000, which aimed at the creation of broader and morphologically more varied recharge basins, and at a rise of water tables in the recharge area to stimulate phreatophytic plant communities. The water table rise resulted in groundwater conditions becoming more anoxic, as evidenced by the increasing Fe, Mn, NH_4 and PO_4 concentrations. This resulted in increasingly more reductive dissolution of iron (hydr)oxides from which the As was inferred to be mobilized. A clear seasonal pattern in this reductive dissolution was observed, showing As peaks in late summer or autumn when temperature is highest and NO_3 lowest due to more denitrification (Stuyfzand et al., 2014).

The upward trend in As concentrations also correlated with a decreasing trend in O_2 concentrations, an upward trend in temperature, HCO_3 and TOC concentrations, and a decreased infiltration rate.
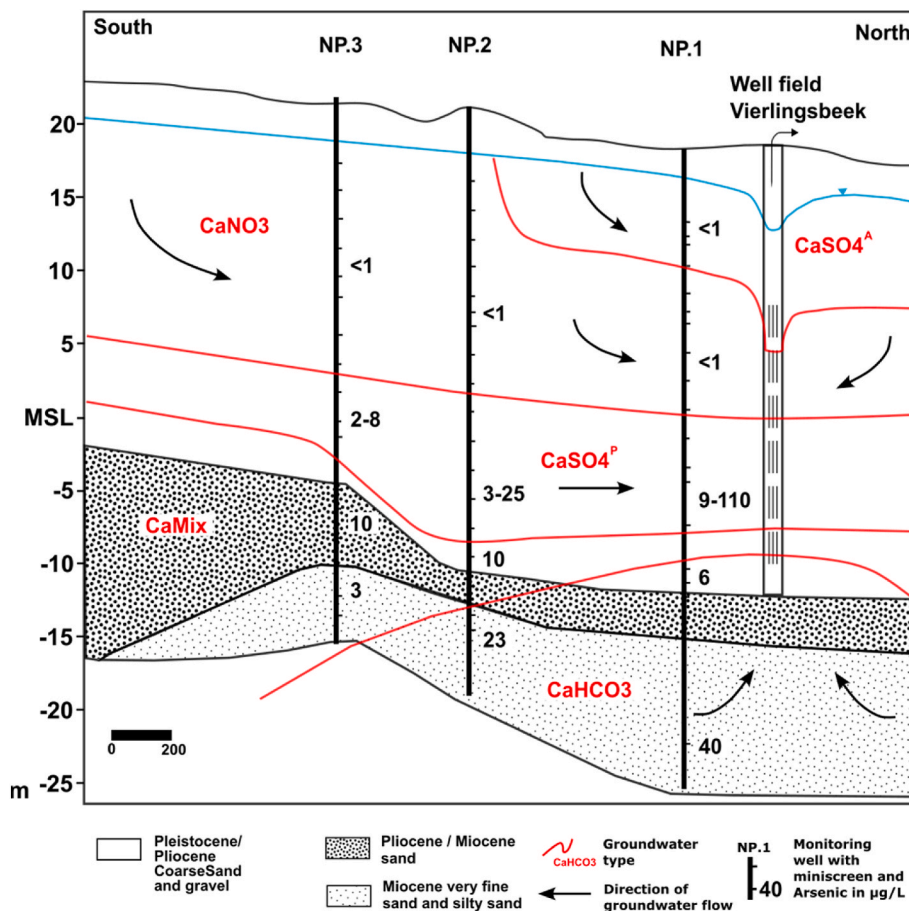
Fig. 9. Site 5: Schematized spatial distribution of chemical water types and As concentrations (in red) in a cross-section across three mini-screened observation wells (NP.1-3) and pumping well 276 of well field Vierlingsbeek, in 1988. SL = Sea Level.

$CaSO_4^A$ = (sub)oxic $CaSO_4$ water with low agricultural inputs and moderate atmospheric SO_4 inputs.

$CaNO_3$ = (sub)oxic $CaNO_3$ water with very high agricultural inputs without denitrification.

$CaSO_4^P$ = anoxic $CaSO_4$ water with high agricultural inputs and high SO_4 deriving from pyrite.

CaMix = transition from $CaSO_4^P$ to $CaHCO_3$.

$CaHCO_3$ = anoxic $CaHCO_3$ water with little or without agricultural impacts.
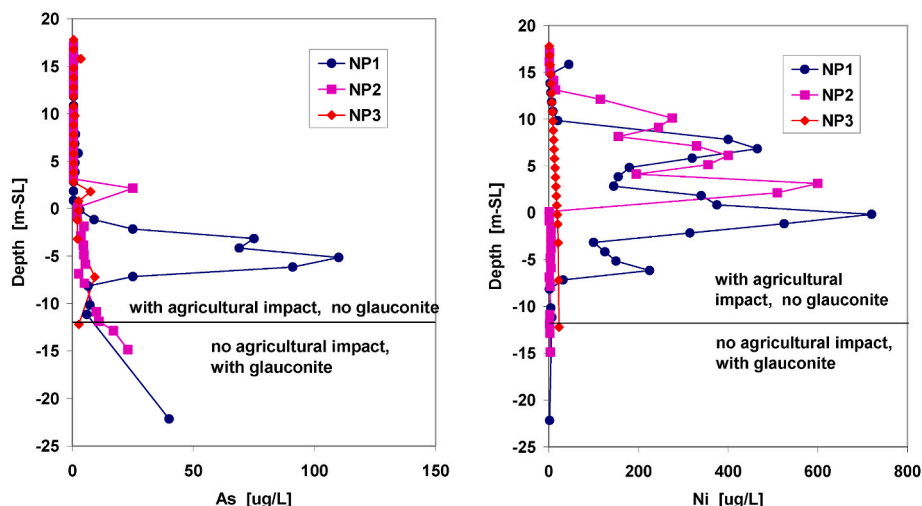
Fig. 10. Site 5: As and Ni depth log of observation wells NP.1-3 in 1988. Left panel modified from Stuyfzand et al. (2008).

Concentrations of As, Fe and PO_4 increased by about the same factor (4) in the period 2000–2013: As from 3 to 13 µg/L, Fe from 0.25 to 1.0 mg/L and PO_4-total from 0.06 to 0.24 mg/L. Mo and V showed a positive correlation with As peaks, in 12 observation wells, contrary to Co and Zn which showed a negative correlation. This indicates that Mo and V (both oxyanions) could be bound to $Fe(OH)_3$ as well, and codissolve with it under reducing conditions.

The above discussed Ouddorp case confirms the insight from the other sites that an As increase is often accompanied by groundwater becoming more anoxic: which can be seen from rising Fe(II), Mn(II), NH_4, PO_4, HCO_3 and DOC concentrations and a decline of O_2, NO_3 and SO_4 concentrations.

3.2.10. Case 10: temperature effects of aquifer thermal energy systems

Over the last two decades, the Netherlands have seen an exploding use of aquifers for aquifer thermal energy storage (ATES). This involves extracting groundwater to heat or cool a building, after which the groundwater is infiltrated back into the same aquifer. This causes
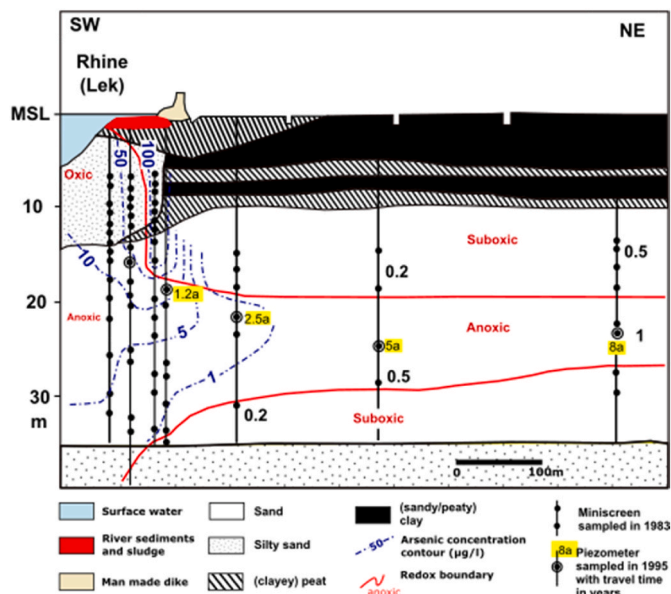
Fig. 11. Site 6: River bank filtrate from the Lek River on site 6, in a (semi) confined, Pleistocene sand aquifer, with iso-concentration lines of total As (modified from Stuyfzand et al., 2006).

temperature perturbations far beyond natural variability. While most systems operate within a range ± 5 °C, there are also applications where much higher groundwater storage temperatures are desirable, between 40 and 60 °C (Bonte, 2015; Fleuchaus et al., 2020; Wesselink et al., 2018). This raised questions regarding groundwater quality impacts, especially when potable aquifers are used (Bonte et al., 2011).

This question was addressed using a column testing setup where aquifer sediments from the Sterksel formation (a Pleistocene sand aquifer used for both drinking water production and ATES) were flushed with ambient anoxic groundwater at various temperatures. This showed that As is very sensitive to temperature change, with the As concentration doubling when temperature is increased from 11 to 25 °C (Bonte et al., 2013a, 2013b). These results were confirmed in several other laboratory studies (Craig, 2018; Javed and Siddique, 2016; Lüders et al., 2020).

Based on leaching patterns observed during the column testing (Bonte et al., 2013a), inferred that As mobilization was caused by desorption from, and potentially reductive dissolution of, iron oxides. Reactive transport modelling was used to simulate these processes. It showed that ATES operation at elevated temperature causes transport of As from the center of the hot zone where it is released to the fringe of the cold zone where it is resorbed (Bonte et al., 2014). This however

assumes a homogeneous geochemical distribution of sorbents, and a more heterogeneous distribution may result in As mobilizing further away from the ATES system.

Water quality data from ATES sites confirms the temperature influence on As concentrations but results are variable. For example at the Koppert-Cress site in the Netherlands where As concentrations decrease as a result of mixing processes (Guglielmetti et al., 2021). At another site in the Netherlands in Wageningen (NIOO) both increasing and decreasing As concentrations with increasing and decreasing temperature are observed (Guglielmetti et al., 2021) which is in line with modelling results by (Bonte et al., 2014). These studies showed that temperature is an important factor influencing As mobility which requires monitoring, especially at systems operating at high temperatures.

3.3. Review of arsenic mobilizing processes in The Netherlands

Based on the collected data and interpretation for these sites, seven processes for arsenic mobilization can be recognized (Table 5). The dissolution of sulfuric arsenic minerals without redox changes (no. D) is not discussed further because of its presumed very rare occurrence in the Netherlands but can be important elsewhere (Kim et al., 2000). A survey of the main triggers, processes and accompanying hydrochemical indicators of arsenic mobilization at the 10 study sites is presented in Table 6.

3.3.1. Process A: desorption by a decreasing Anion Exchange Capacity

Several processes can negatively influence the Anion Exchange Capacity (AEC) of minerals present in the aquifer system. This may occur when iron and aluminum (hydr)oxides dissolve or ripen into higher crystallinities (Smedley and Kinniburgh, 2002). The ripening of hydrous ferric oxides (HFO) to more crystalline minerals such as goethite (α-FeOOH) results in a decrease in surface area and desorption of anions like arsenate (Dixit and Hering, 2003; Stolze et al., 2019). This is illustrated by the chemical composition of mineral deposits found in water well screens, showing decreasing As content when HFO ripen to higher crystallinities (Houben and Treskatis, 2007). Ripening of HFO, can also result in incorporation of As into the crystal lattice and become more firmly incorporated to the product phase (Pedersen et al., 2006). We presume that this process is also active in specific groundwater flow systems, for instance where groundwater tables first decline, with concomitant HFO formation from oxidizing pyrite. When groundwater levels are restored, recently formed HFO may reductively re-dissolve (Burton et al., 2014). Released Fe^{2+} may be flushed to other parts of the aquifer where HFO is transformed to goethite or hematite. This may have happened on sites where groundwater extraction was followed by artificial recharge like in the coastal dunes (Site 3).
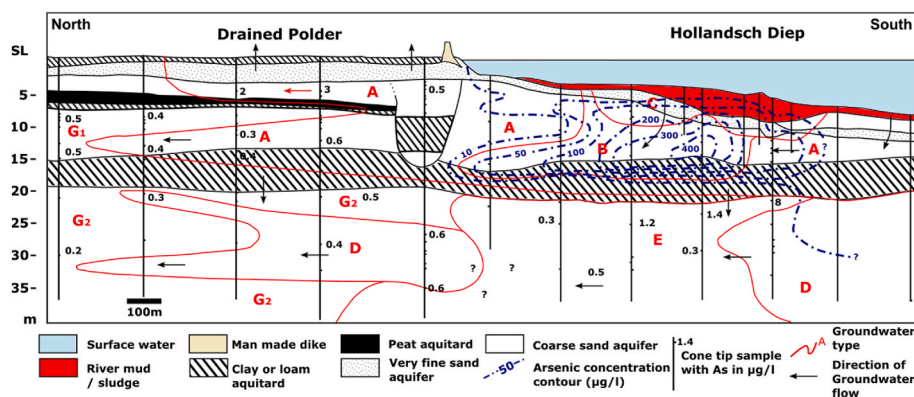

Fig. 12. Site 7: Distribution of arsenic concentrations and generic groundwater types A-G in river bank filtrate in the Hollandsch Diep estuary. Samples taken in 1997.
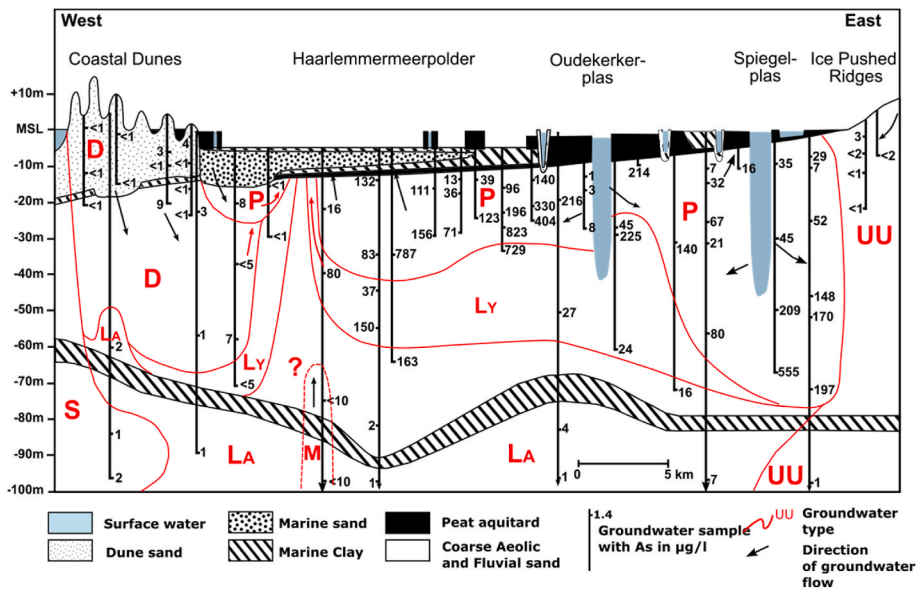
Fig. 13. Site 8. West-east cross section (see Fig. 1 for location) over the high As-belt south of Amsterdam, showing the spatial distribution of water bodies, groundwater flow direction and As concentrations in monitoring wells [µg/L]. Modified from Van Rossum (unpublished). Groundwater types: D: Dune hydrosome (fresh); P: Polder hydrosome (fresh); UU Upland hydrosome (fresh); S: North sea hydrosome (saline); L_Y: Lagoonal and tidal flat hydrosome, young (fresh to brackish); LA: Lagoonal and tidal flat hydrosome, ancient (brackish to saline); M: Maassluis hydrosome (brackish to saline).
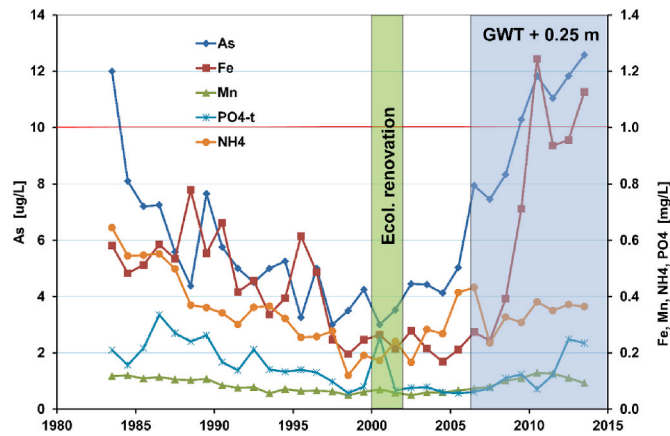
Fig. 14. Annual mean concentrations of As, Fe, Mn, NH_4 and PO_4 in the period 1983–2013, for the raw water recovered from artificial recharge area Ouddorp (From Stuyfzand et al., 2014).

3.3.2. Process B: Anion exchange

Arsenic, especially when sorbed as arsenate on iron (hydr)oxides, can be exchanged with ions such as PO_4 (Holm, 2002; Islam and Mostafa, 2021; Manning and Goldberg, 1996; Ngantcha-Kwimi and Reed, 2020), HCO_3 (Anawar et al., 2004; Appelo, 2008; Appelo et al., 2002; Holm, 2002), SO_4 (Ghurye et al., 1999; Xu et al., 1988), F (Wu et al., 2017), H_4SiO_4 (Nguyen et al., 2011; Swedlund and Webster, 1999), and possibly DOC (Malik et al., 2020; Smedley and Kinniburgh, 2002). Such competition induced As desorption can be expected in situations where a change in water management (for example artificial recharge) resulted in the introduction of water with increased PO_4, HCO_3, H_4SiO_4 and DOC concentrations in aquifers with ambient groundwater with relative low concentrations of these species (Sites 3, 6–8), or in situations where an increase in these species is generated by increasingly reducing conditions and reductive dissolution of Fe-oxides (Site 6).

Changes in anion sorption selectivity or the point of zero charge of the sorbent may also induce As desorption. These changes can be due to changes in salinity, pH or temperature (Bonte et al., 2013a; Ghurye et al., 1999; Kersten and Vlasova, 2009). This is likely a main contributor for As mobilization for the ATES column tests at site 10. Elevated SO_4 concentrations may contribute to the high As levels on site 5 which is characterized by a low pH (4.6–5.3). The infiltration of polluted surface

Table 5

Overview of the most probable arsenic mobilizing processes, their triggering and estimated incidence in the Netherlands.1-4 without, 5–7 with redox reactions. AEC = Anion Exchange Capacity; SOM = Soil Organic Material; DOC = Dissolved Organic Carbon.

No.	Mobilizing process	Trigger	Freq[1]
A	Desorption by decreasing AEC	Ripening of iron(hydr)oxides (Fe^{2+} flushing, Time, Temp increase); Increase of pH and Temp; Clay + peat compaction?	C
B	Anion exchange	Flushing with higher conc of PO_4, H_4SiO_4, HCO_3, DOC, SO_4, F, I; Changes in selectivity of sorbent	CC
C	Dissolution of minerals containing As traces (like phosphorite, apatite, struvite)	Flushing of anoxic system with lower pH and lower conc of PO_4, Fe^{2+}, CO_3, etc.	C
D	Dissolution of As-minerals (like As_2S_3)	Flushing of anoxic system with higher conc of CO_3^{2-} which raises solubility by complexes as As $(CO_3)_2$, $As(CO_3)(OH)_2$, $AsCO_3^+$	RR
E	Oxidation of Fe-sulfide minerals	Moderate input of O_2 and/or high input of NO_3 with Fe^{2+} (partly) escaping from oxidation; Lowering of groundwater table	CC
F	Reduction of H_3AsO_4 to H_3AsO_3	High input of CH_4, H_2, labile DOC, H_2S (Fe^{2+} low); Contact with SOM; Inundation or rise of groundwater table;	CC
G	Reductive dissolution of iron (hydr)oxides		CC

Note: C = frequent; CC = very frequent; RR = very rare.

waters also increased SO_4 and F concentrations in AR and RBF systems, but the pH of these waters is probably too high (7–8) and the concentration increase relatively limited (up to 100 mg/L SO_4 and 0.4 mg/L F) for SO_4 and F to become a significant As desorbent.

Artificial recharge with surface water and saturated with respect to calcite at Sites 3 and 4, resulted in increases in groundwater pH from 7.3 to 7.8 (Stuyfzand, 1993b). This may have contributed to mobilizing As at these sites. Fresh groundwater intrusions into brackish or saline aquifers often lead to more pronounced pH increases (from 7.5 to 8–8.5; (Stuyfzand, 1993a), but no As mobilization has been observed there. This may indicate that As sorption to reactive surfaces is limited in these strongly reducing environments.

Table 6

Survey of arsenic occurrence at the 10 study sites, main triggers and accompanying redox conditions.

Site		As-max			Conditions		
No.	Name	µg/L	Depth [m-LS]	Age [a]	Main processes #	Main triggers ##	Redox
1	Zandvoort dunes	2–10	9	5–10	G	Redox transition	Oxic/suboxic
2	West-Brabant uplands	25–40	175	2000–10,000	C	GMA, Ca-adsorption?	anoxic
3	AR Basin, Zandvoort	50	13	4–20	E,F,G,A	ARB, GWT down & up	suboxic
4	AR DWI, Langerak	90	92	0.02–0.5	E	DWI	suboxic
5	Vierlingsbeek	110	27	30–40	E, B	excessive manuring, GWT down	suboxic
6	RBF Opperduit	200	5–15	0.2–4	G, F,C,B	deposition mud	anoxic
7	RBF Hollandsch Diep	420	12–15	5–25	G, F,C,B	deposition mud; struvite diss?	anoxic
8	Polders south of Amsterdam	880	30	20–200	G,F,E,C,B,A	drainage, peat excavation and sand pits	anoxic
9	AR Basin, Ouddorp	27	2–4	0.3–5	G,F	rise of water table	suboxic
10	ATES Laboratory experiments, Scherpenzeel	138	35	NA	G,F,A	rise of temperature	suboxic/ anoxic

Notes: #: number corresponding with Table 6, in order of decreasing importance; ##: ARB = Artificial recharge via basins, using oxic water; DWI = Deep well injection into anoxic aquifer, using oxic water; GMA = dissolution glauconite mineral assemblage; GWT = Groundwater table; RBF = River bank filtration; R: relative retardation factor = time of Ni peaking since infiltration/time of As peaking since infiltration.

3.3.3. Process C: dissolution of non-sulfuric mineral phases containing as traces

The most important As containing non-sulfuric mineral phases in the Netherlands, are probably contained in anoxic glauconitic sands and clays of Pliocene and Miocene age (Site 2), and in recent underwater muds and sludge (Site 6–7). The exact non-sulfuric sources of As in these sediments are not clear. However, in the glauconitic sediments it could be the anoxic weathering of glauconite or of associated minerals like apatite and carbonates. As a large fraction of the As is not S-bound (Supplementary Information), it is hypothesized that cation exchange due to fresh water intrusion, which depletes Ca and raises Na, K and Mg, may also trigger the dissolution of apatites and carbonates which have

As associated. Struvite could be present in the polluted underwater muds and sludge on Site 7. The mineral saturation index of water type C (sample 37 in Table 4) with respect to struvite is indeed close to 0, indicating that the water approaches saturation possibly by dissolving struvite.

3.3.4. Process E: redox reactions: pyrite oxidation

Oxidation of pyrite is one of the most important As mobilizing process in the Netherlands, especially in closed systems exposed to nitrate pollution. This situation occurs at Site 5 with high agricultural NO_3 input (Fig. 9), and at Site 4 where oxic drinking water is injected. The relevant chemical reactions are schematized as equations 7-10 in

Table 7

Overview of the most important redox reactions with organic material, pyrite and ferrihydrite, and the resulting concentration changes in water for inorganic carbon species, nutrients and trace constituents of the reacting solid phases. Reactions generating the highest concentrations of trace elements and nutrients show a-h without brackets in blue cells. Reactions showing a-h within brackets indicate that the mobilized nutrients or trace elements are largely immobilized by secondary reactions (chemisorption to $Fe(OH)_3$ or nitrification).

No.	Equation	CO₂	HCO₃	TIC $	NH₄	PO₄	I	As	Co	Ni	Zn
	Reaction				**Concentration change [mol/L] on the product side ##**						
	Oxidation of organic material (CH₂O)										
1	$CH_2O + O_2 \rightarrow CO_2 + H_2O$	1	0	2	(a)	(b)	(c)	0	0	0	0
2	$CH_2O + 0.8\ NO_3^- \rightarrow 0.4\ N_2 + 0.2\ CO_2 + 0.8\ HCO_3 + 0.6\ H_2O$	0.2	0.8	1.2	(a)	(b)	(c)	0	0	0	0
3	$CH_2O + 4\ Fe(OH)_3 + 7\ CO_2 \rightarrow 4\ Fe^{2+} + 8\ HCO_3^- + 3\ H_2O$	-7	8	1	a	b	c	?	0	0	0
4	$CH_2O + 0.5\ SO_4^{2-} \rightarrow 0.5\ H_2S + HCO_3^-$	0	1	1	a	b	c	0	0	0	0
5	$CH_2O + 0.5\ CO_2 \rightarrow 0.5\ CH_4 + CO_2$	0.5	0	1	a	b	c	0	0	0	0
6	$CH_2O + 2\ H_2O \rightarrow 2\ H_2 + CO_2 + H_2O$	1	0	2	a	b	c	0	0	0	0
	Oxidation of pyrite (FeS₂)										
7	$FeS_2 + 3.5\ O_2 + 2\ HCO_3^- \rightarrow Fe^{2+} + 2\ SO_4^{2-} + 2\ CO_2 + H_2O$	2	-2	2	0	0	0	e	f	g	h
8	$FeS_2 + 3.75\ O_2 + 4\ HCO_3^- \rightarrow Fe(OH)_3 + 2\ SO_4^{2-} + 4\ CO_2 + 0.5\ H_2O$	4	-4	4	0	0	0	(e)	(f)	(g)	(h)
9	$FeS_2 + 2.8\ NO_3^- + 0.8\ CO_2 + 0.4\ H_2O \rightarrow Fe^{2+} + 2\ SO_4^{2-} + 0.8\ HCO_3^- + 1.4\ N_2$	-0.8	0.80	0	0	0	0	e	f	g	h
10	$FeS_2 + 3\ NO_3^- + HCO_3^- + H_2O \rightarrow Fe(OH)_3 + 2\ SO_4^{2-} + CO_2 + 1.5\ N_2$	1	-1	1	0	0	0	(e)	(f)	(g)	(h)
	Reduction of ferrihydrite (Fe(OH)₃)										
11	$Fe(OH)_3 + 0.25\ CH_2O + 1.75\ CO_2 \rightarrow Fe^{2+} + 2\ HCO_3^- + 0.75\ H_2O$	1.75	2	0.25	a	b	c	?	0	0	0
12	$Fe(OH)_3 + ⅛\ H_2S + 1.75\ CO_2 \rightarrow Fe^{2+} + ⅛\ SO_4^{2-} + 1.75\ HCO_3^- + 0.75\ H_2O$	-1.75	1.75	0	0	0	0	?	0	0	0
13	$Fe(OH)_3 + ⅛\ CH_4 + 1.88\ CO_2 \rightarrow Fe^{2+} + 2\ HCO_3^- + 0.75\ H_2O$	-1.875	2	0.125	0	0	0	?	0	0	0
14	$Fe(OH)_3 + 0.5\ H_2 + 2\ CO_2 \rightarrow Fe^{2+} + 2\ HCO_3^- + H_2O$	-2	2	0	0	0	0	?	0	0	0

Notes: ## = upon oxidation of 1 mol/L CH2O or FeS2, or reduction of 1 mol/L Fe(OH)3, assuming conservative behavior of trace constituents (NH4, PO4, I, As, Co, Ni, Zn); $ = Total Inorganic Carbon, assuming all CO2 reacting with CaCO3; a, b = average molar content of CH2O according to resp. Froelich et al. 1979 and Ullman & Aller 1985: a = 0.075-0.151 NH4, b = 0.0045-0.0094 PO4; c = average molar content of CH2O according to Ullman & Aller 1985: 0.0002 I-total

e, f, g, h = average molar content of FeS2 (Table 4): e = 0.0018-0.0058, f = 0.0003-0.0048, g = 0.0013-0.0145, h = 0.0029-0.0421

Table 7.

At both sites pyrite oxidation is clearly demonstrated by the complete loss of oxidants, the stoichiometric release of SO_4, and the (temporal) mobilization of As, Co and Ni. At Site 5, with pH 4.5–5.4 due to natural decalcification and high acid inputs (by nitrification and pyrite oxidation), Co and Ni concentrations approximate the stoichiometric pyrite oxidation, whereas As and Fe show a smaller release due to neo-formation of HFO and increasing As sorption at low pH.

During deep well injection at Site 4, As was mobilized close to its stoichiometric release only in the beginning and close to the injection well, when O_2 and NO_3 were firstly introduced to pyritiferous deposits (Fig. 7). As injection at this site continued, released Fe^{2+} was converted to HFO that sorbed mobilized As and dampened aqueous concentrations. When redox conditions in the aquifer become less reducing, arsenite may be oxidized to arsenate, subject to availability of O_2 or NO_3, which can depending on prevailing pH influence overall arsenic mobility (Dixit and Hering, 2003).

The downstream attenuation of As plume is probably connected with continued HFO interaction. The latter could be transported as colloidal particles over a limited distance before being deposited when either the velocity of groundwater flow reduces or where sediments become finer resulting in trapping of colloidal particles. In fact, anoxic filtration of the water samples in the field led to a remarkable removal of ferric iron flocs, as evidenced by a brownish coating of the membrane filters used. This particle transport in deep well injection systems is enhanced by relatively high groundwater flow velocities (1–3 m/d). When compared to Site 5, deep well injection resulted in higher As and lower Co, Ni and Zn concentrations. This is attributed to the higher pH (7.3), which raises the mobility of As and decreases the mobility of Co, Ni and Zn. Pyrite oxidation may have played an indirect role at Sites 1 and 3, where the groundwater table first declined (and pyrite oxidized) and was later restored.

3.3.5. Process F: redox reactions leading to reductive dissolution

Reductive dissolution of iron (hydr)oxides with the reduction of arsenate to the more mobile arsenite forms the second most important As mobilization process in the Netherlands. The reduction is mainly achieved in the upper 300 m where fresh groundwater is pumped for drinking water supply, by unstabilized soil organic matter (SOM), either directly in solid or dissolved state (reaction 11 in Table 7), or indirectly through the gases H_2S, CH_4 and H_2 (reactions 12–14 in Table 7). These gases are produced during either fermentation of SOM or oxidation of SOM coupled with sulfate reduction (reactions 4–6 in Table 7).

Although anaerobic oxidation of methane by ferrihydrite (reaction 13) has been reported to occur under natural conditions (Cornell and Schwertmann, 2003), no data on the reaction kinetics at ambient temperatures were found in the literature, indicating that further research on the relevance of reaction 13 is needed. SOM is represented in the above-mentioned reactions as $CH_2O(NH_3)_W(H_3PO_4)_yI_z$ with default values w = 0.151 and y = 0.0091 in accordance with (Froelich et al., 1979), or w = 0.075 and y = 0.0045 in accordance with Hartmann et al. (1973), and z = 0.0002 in accordance with (Ullman and Aller, 1985).

Methane concentrations in anoxic groundwaters in the Netherlands are normally in the range of 1–50 mg/L, with occasional outliers to 100 mg/L (Cirkel et al., 2015; Fortuin and Willemsen, 2005; Stuyfzand, 1994). Reaction 5 shows that the presence of methane should be associated with high concentrations of HCO_3, NH_4, PO_4 and I. This is indeed very often the case (Stuyfzand, 1993b, 1994), which also holds for dissolved organic carbon (DOC). The para-genesis of CH_4, CO_2, HCO_3, NH_4, PO_4, DOC and I implies that mobilized arsenite, if it could sorb anyway, finds a huge amount of competitors (PO_4, HCO_3, DOC and I) which increases its mobility. It should be noted that the direct reduction of Fe $(OH)_3$ by labile organic material likewise yields elevated concentrations of at least HCO_3, NH_4 and PO_4 (Reaction 3). It can therefore be concluded that redox reactions in a reducing (suboxic to anoxic) environment, not only dissolve iron (hydr)oxides and the associated As, but

also generate anions and DOC that act as inhibitors of As sorption. In addition, high concentrations of H_4SiO_4 may develop in anoxic environments due to the dissolution of diatoms, which can be abundant in the aquitards responsible for developing the anoxic conditions (Stuyfzand, 1993b).

Unfortunately very strong correlations do not exist between As and single indicators of anoxic conditions (like high CH_4, HCO_3, NH_4, PO_4, and DOC concentrations and low SO_4 contents) (for instance (Appelo, 2008; Smedley and Kinniburgh, 2002)). This is due to many secondary processes taking place when large amounts of SOM, $CaCO_3$ and iron (hydr)oxides dissolve. These processes include CH_4 bubble migration, sorption of Fe^{2+}, NH_4, As, PO_4 and DOC, and precipitation of minerals like siderite, apatite and vivianite, which may sequester As again. (Postma et al., 2007) noted a good positive correlation between As and NH_4 which is not evident for data presented in Table 4, where NH_4 and As have a correlation coefficient of less than 0.04. This indicates that the use of indicator parameters is strongly restricted to the aquifer for which the data are collected and care should be taken to extrapolate such to other geochemical systems.

4. Implications and conclusions

Although our review showed that elevated As concentrations may occur in various groundwater systems in the Netherlands, no major As problems have been encountered in drinking water supply. Arsenic concentrations in most fresh groundwater systems in the Netherlands are low (<10 μg/L), as observed at Site 1 (coastal dunes). This is considered representative for most sandy recharge areas under natural conditions without large scale hydrologic disturbances. At sites where higher As concentrations are present in raw groundwater, water treatment effectively reduces arsenic concentrations. This usually involves aeration followed by rapid sand filtration resulting in precipitation of iron(hydr)oxides and co-precipitation of As (Ahmad, 2020, de Moel et al., 2006). Recently, the Dutch drinking water sector has aimed at increasing water treatment efforts further to meet a drinking water criterion of <1 μg/l, which is a factor of 10 lower than the WHO health advisory limit (Ahmad et al., 2020b). This is achievable through further optimization of Fe based co-precipitation methods (Ahmad et al., 2020a).

Our review highlighted that elevated arsenic concentrations are present in a wide range of hydrogeological conditions under anthropogenic pressures. Understanding the hydrochemical processes and anthropogenic influences that trigger these processes is key to predicting future trends in arsenic concentrations in groundwater. Our review identified a number of systems where elevated As may occur: 1) Groundwater extraction from aquifers in anoxic glauconitic deposits of upper Tertiary age (As concentrations up to 40 μg/L); 2) Systems where surface water is used for artificial recharge via basins (max. 50 μg/L) or wells (max. 90 μg/L); 3) Systems with pyritiferous sediments under pressure of nitrate pollution (max. 110 μg/L); 4) Aquifers fed by surface water bodies where infiltrating water passes accumulated underwater muds and sludge (max. 420 μg/L); 5) Man-made polders and reclaimed lakes south of Amsterdam (max. 880 μg/L). Anthropogenic temperature perturbations, for example caused by aquifer thermal energy storage, have the potential to raise As concentrations (site 10).

This study suggests that the most severe As problems in the Netherlands relate to interactions of (occasionally) polluted surface water and groundwater (as in AR and RBF systems), especially where redox conditions are variable through time, for example changing from reducing to oxidizing and then back to reducing, or where methanogenic polluted underwater muds and sludge interfere with groundwater recharge. Interestingly, these findings are partly in line with those reported by (Harvey et al., 2006) who identified intensified groundwater flow, increasing aquifer recharge via ponds and rivers, and inputs of labile organic carbon via waste water as main drivers for arsenic problems in Bangladesh.

Author contribution

PS carried out the data collection and interpretation for sites 1–9, MB for site 10. PS and MB jointly wrote and edited the manuscript.

Declaration of competing interest

The authors declare that they have no known competing financial interests or personal relationships that could have appeared to influence the work reported in this paper.

Data availability

The data that has been used is confidential.

Appendix A. Supplementary data

Supplementary data to this article can be found online at https://doi.org/10.1016/j.apgeochem.2023.105596.

References

Ahmad, A., 2020. Arsenic Removal by Iron Based Co-precipitation : Mechanisms in Groundwater Treatment, vol. 96. Wageningen University. Sectie Milieutechnologie.

Ahmad, A., Heijnen, L., de Waal, L., Battaglia-Brunet, F., Oorthuizen, W., Pieterse, B., Bhattacharya, P., van der Wal, A., 2020a. Mobility and redox transformation of arsenic during treatment of artificially recharged groundwater for drinking water production. Water Res. 178, 115826 https://doi.org/10.1016/J.WATRES.2020.115826.

Ahmad, A., Kools, S., Schriks, M., Stuyfzand, P., Hofs, B., 2015. Arsenic and Chromium Concentrations and Their Speciation in Groundwater Resources and Drinking Water Supply in the Netherlands. KWR.

Ahmad, A., van der Wens, P., Baken, K., de Waal, L., Bhattacharya, P., Stuyfzand, P., 2020b. Arsenic reduction to <1 μg/L in Dutch drinking water. Environ. Int. 134, 105253 https://doi.org/10.1016/J.ENVINT.2019.105253.

Anawar, H.M., Akai, J., Sakugawa, H., 2004. Mobilization of arsenic from subsurface sediments by effect of bicarbonate ions in groundwater. Chemosphere 54. https://doi.org/10.1016/j.chemosphere.2003.08.030.

Appelo, C.A.J., 2008. Geochemical Experimentation and Modeling Are Tools for Understanding the Origin of as in Groundwater in Bangladesh and Elsewhere, vol. 5. Arsenic in Groundwater—A World Problem; NNC-IAH Pub., Utrecht, The Netherlands, pp. 33–50.

Appelo, C.A.J., Van Der Weiden, M.J.J., Tournassat, C., Charlet, L., 2002. Surface complexation of ferrous iron and carbonate on ferrihydrite and the mobilization of arsenic. Environ. Sci. Technol. 36 https://doi.org/10.1021/es010130n.

Banning, A., 2021. Geogenic arsenic and uranium in Germany: large-scale distribution control in sediments and groundwater. J. Hazard Mater. 405 https://doi.org/10.1016/j.jhazmat.2020.124186.

Bonte, M., Stuyfzand, P.J., Hulsmann, A., van Beelen, P., 2011. Underground thermal energy storage: environmental risks and policy developments in The Netherlands and European Union. Ecol. Soc. 16 https://doi.org/10.5751/ES-03762-160122.

Bonte, M., van Breukelen, B.M., Stuyfzand, P.J., 2013a. Temperature-induced impacts on groundwater quality and arsenic mobility in anoxic aquifer sediments used for both drinking water and shallow geothermal energy production. Water Res. 47 https://doi.org/10.1016/j.watres.2013.05.049.

Bonte, M., Van Breukelen, B.M., Stuyfzand, P.J., 2013b. Environmental impacts of aquifer thermal energy storage investigated by field and laboratory experiments. Journal of Water and Climate Change 4. https://doi.org/10.2166/wcc.2013.061.

Bonte, M., Stuyfzand, P.J., Breukelen, B.M.V., 2014. Reactive transport modeling of thermal column experiments to investigate the impacts of aquifer thermal energy storage on groundwater quality. Environ. Sci. Technol. 48 https://doi.org/10.1021/es502477m.

Bonte, M., 2015. Impacts of Shallow Geothermal Energy on Groundwater Quality. IWA Publishing, London. https://doi.org/10.2166/9781780406824.

Broers, H.P., Buijs, E.A., 1997. Origin of Trace Metals and Arsenic at the Oostrum Well Field (In Dutch). Utrecht doi.org/Report NITG 97-189-A.

Brunt, R., Vasak, L., Griffioen, J., 2004. Arsenic in Groundwater: Probability of Occurrence of Excessive Concentration on Global Scale. International Groundwater Resources Centre (IGRAC) Delft.

Bundschuh, J., Bhattacharya, P., Chandrashekharam, 2005. Natural Arsenic in Groundwater: Occurrence, Remediation and Management. Science of The Total Environment - SCI TOTAL ENVIR. https://doi.org/10.1201/9780203970829.ch3

Burton, E.D., Johnston, S.G., Kocar, B.D., 2014. Arsenic mobility during flooding of contaminated soil: the effect of microbial sulfate reduction. Environ. Sci. Technol. 48 https://doi.org/10.1021/es503963k.

Chakraborty, M., Mukherjee, A., Ahmed, K.M., 2022. Regional-scale Hydrogeochemical Evolution across the Arsenic-Enriched Transboundary Aquifers of the Ganges River Delta System, India and Bangladesh, vol. 153490. Science of The Total Environment. https://doi.org/10.1016/J.SCITOTENV.2022.153490.

Cirkel, G., Hartog, N., De La, B., Gonzalez, L., Stuyfzand, P., 2015. Methaan in ondiep Nederlands grondwater: Verbinding met de diepe ondergrond. H2O online.

Coetsiers, M., 2007. Research into the hydrogeological and hydrochemical conditions of the Neogene aquifer in Flanders, using modeling and isotope hydrochemistry. In: Dutch. Ghent University. PhD Univ Ghent (Belgium).

Coetsiers, M., Walraevens, K., 2006. Chemical characterization of the neogene aquifer, Belgium. Hydrogeol. J. 14 https://doi.org/10.1007/s10040-006-0053-0.

Cornell, R.M., Schwertmann, U., 2003. The Iron Oxides: Structure, Properties, Reactions, Occurrences and Uses, second ed. WILEY-VCH GmbH&Co. KGaA.

Coudert, L., Bondu, R., Rakotonimaro, T.V., Rosa, E., Guittonny, M., Neculita, C.M., 2020. Treatment of As-rich mine effluents and produced residues stability: current knowledge and research priorities for gold mining. J. Hazard Mater. 386, 121920 https://doi.org/10.1016/J.JHAZMAT.2019.121920.

Craig, A.T., 2018. Using Heated Column Experiments to Investigate the Effects of In-Situ Thermal Recovery Operations on Groundwater Geochemistry in Cold Lake. PhD Thesis. Carleton University, Alberta.

Cremer, N., Obermann, P., Wisotzky, F., 2003. Mobilization of Nickel, Cobalt and arsenic in a multi-aquifer formation of the Lower-Rhine valley: identification and modeling of the processes controlling metal mobility. In: Schulz, H.D., Hadeler, A. (Eds.), Geochemical Processes in Soil and Groundwater: Measurement, Modelling and Upscaling. Deutsche Forschungsgemeinschaft, pp. 3–18.

de Moel, P.J., Verberk, J.Q.J.C., van Dijk, J.C., 2006. Drinking water: principles and practices, drinking water: principles and practices. https://doi.org/10.1142/6135.

Dean, W.E., 1974. Determination of carbonate and organic matter in calcareous sediments and sedimentary rocks by loss on ignition: comparison with other methods. J. Sedim. Petrol. 44, 242–248.

Dehbandi, R., Abbasnejad, A., Karimi, Z., Herath, I., Bundschuh, J., 2019. Hydrogeochemical controls on arsenic mobility in an arid inland basin, Southeast of Iran: the role of alkaline conditions and salt water intrusion. Environ. Pollut. 249 https://doi.org/10.1016/j.envpol.2019.03.082.

Dixit, S., Hering, J.G., 2003. Comparison of arsenic(V) and arsenic(III) sorption onto iron oxide minerals: implications for arsenic mobility. Environ. Sci. Technol. 37 https://doi.org/10.1021/es030309t.

Donovan, J.J., Grimm, E.C., 2007. Episodic struvite deposits in a Northern Great Plains flyway lake: indicators of mid-Holocene drought? Holocene 17. https://doi.org/10.1177/0959683607082556.

Engelen, J.M.E., 1986. Water systems in The Netherlands. In: Engelen, G.B., P, J.G. (Eds.), Developments in the Analysis of Groundwater Flow Systems; A Contribution to IHP Project A.2.8. IAHS, p. 356.

Fleuchaus, P., Schüppler, S., Bloemendal, M., Guglielmetti, L., Opel, O., Blum, P., 2020. Risk analysis of high-temperature aquifer thermal energy storage (HT-ATES). Renew. Sustain. Energy Rev. 133 https://doi.org/10.1016/j.rser.2020.110153.

Flink, J., 1985. The distribution of arsenic in the groundwater of the southern parts of the province of Noord-Brabant. RIVM Rapport, 840348004 (in Dutch).

Fortuin, N.P.M., Willemsen, A., 2005. Exsolution of nitrogen and argon by methanogenesis in Dutch ground water. J. Hydrol. (Amst.) 301. https://doi.org/10.1016/j.jhydrol.2004.06.018.

Froelich, P.N., Klinkhammer, G.P., Bender, M.L., Luedtke, N.A., Heath, G.R., Cullen, D., Dauphin, P., Hammond, D., Hartman, B., Maynard, V., 1979. Early oxidation of organic matter in pelagic sediments of the eastern equatorial Atlantic: suboxic diagenesis. Geochem. Cosmochim. Acta 43. https://doi.org/10.1016/0016-7037(79)90095-4.

Ghurye, G.L., Clifford, D.A., Tripp, A.R., 1999. Combined arsenic and nitrate removal by ion exchange. J. Am. Water Works Assoc. 91 https://doi.org/10.1002/j.1551-8833.1999.tb08718.x.

Guglielmetti, L., Bloemendal, M., Hahn, F., Koornneef, J., Hilleke Mortensen, M., 2021. Environmental Effects of UTES Technologies in Europe.

Hartmann, M., Müller, P., Suess, E., Van der Weijden, C.H., 1973. Oxidation of organic matter in recent marine sediments. Meteor Forsch.-Ergebnisse, Reihe C 12, 74–86.

Harvey, C.F., Ashfaque, K.N., Yu, W., Badruzzaman, A.B.M., Ali, M.A., Oates, P.M., Michael, H.A., Neumann, R.B., Beckie, R., Islam, S., Ahmed, M.F., 2006. Groundwater dynamics and arsenic contamination in Bangladesh. Chem. Geol. 228 https://doi.org/10.1016/j.chemgeo.2005.11.025.

Heinrichs, G., Udluft, P., 1999. Natural arsenic in Triassic rocks: a source of drinking-water contamination in Bavaria, Germany. Hydrogeol. J. 7 https://doi.org/10.1007/s100400050219.

Hem, J.D., 1985. Study and Interpretation of the Chemical Characteristics of Natural Water. US Geological Survey Water-Supply Paper 2254.

Herath, I., Vithanage, M., Bundschuh, J., Maity, J.P., Bhattacharya, P., 2016. Natural arsenic in global groundwaters: distribution and geochemical triggers for mobilization. Curr Pollut Rep. https://doi.org/10.1007/s40726-016-0028-2.

Holm, T.R., 2002. Effects of CO32–/bicarbonate, Si, and PO43–on Arsenic sorption to HFO. J. Am. Water Works Assoc. 94, 174–181.

Hossain, M.F., 2006. Arsenic contamination in Bangladesh—an overview. Agric. Ecosyst. Environ. 113, 1–16. https://doi.org/10.1016/J.AGEE.2005.08.034.

Houben, G., Treskatis, C., 2007. Water Well Rehabilitation and Reconstruction. McGraw-Hill Education.

Houben, G.J., Sitnikova, M.A., Post, V.E.A., 2017. Terrestrial sedimentary pyrites as a potential source of trace metal release to groundwater - a case study from the Emsland, Germany. Appl. Geochem. 76 https://doi.org/10.1016/j.apgeochem.2016.11.019.

Huisman, D., 1998. Geochemical Characterization of Subsurface Sediments in the Netherlands. Prof.Dr. S.B. Kroonenberg (Supervisor); Dr. G.T. Klaver, dr.Ir. A. veldkamp (co-supervisors) Wageningen Agricultural University, The Netherlands (1998) 175 pp. ISBN 90-54858613.

Huisman, P., Cramer, W., van Ee, G., Hooghart, J.C., Salz, H., Zuidema, F.C., 1998. Water in the Netherlands. Netherlands Hydrol. Soc. (NHV), Delft.

Huq, M.E., Fahad, S., Shao, Z., Sarven, M.S., Khan, I.A., Alam, M., Saeed, M., Ullah, H., Adnan, M., Saud, S., Cheng, Q., Ali, S., Wahid, F., Zamin, M., Raza, M.A., Saeed, B., Riaz, M., Khan, W.U., 2020. Arsenic in a groundwater environment in Bangladesh: occurrence and mobilization. J. Environ. Manag. 262, 110318 https://doi.org/10.1016/J.JENVMAN.2020.110318.

Islam, MdS., Mostafa, M.G., 2021. Influence of chemical fertilizers on arsenic mobilization in the alluvial Bengal delta plain: a critical review. J. Water Supply Res. Technol. - Aqua 70, 948–970. https://doi.org/10.2166/aqua.2021.043.

Javed, M.B., Siddique, T., 2016. Thermally released arsenic in porewater from sediments in the cold lake area of alberta, Canada. Environ. Sci. Technol. 50, 2191–2199. https://doi.org/10.1021/acs.est.5b04555.

Jessen, S., Postma, D., Thorling, L., Müller, I., Leskelä, J., Engesgaard, P., 2017. Decadal variations in groundwater quality: a legacy from nitrate leaching and denitrification by pyrite in a sandy aquifer. Water Resour. Res. 53 https://doi.org/10.1002/2016WR018995.

Jia, Y., Guo, H., Xi, B., Jiang, Y., Zhang, Z., Yuan, R., Yi, W., Xue, X., 2017. Sources of groundwater salinity and potential impact on arsenic mobility in the western Hetao Basin, Inner Mongolia. Sci. Total Environ. 601–602. https://doi.org/10.1016/j.scitotenv.2017.05.196.

Johannesson, K.H., Tang, J., 2009. Conservative behavior of arsenic and other oxyanion-forming trace elements in an oxic groundwater flow system. J. Hydrol. (Amst.) 378, 13–28. https://doi.org/10.1016/J.JHYDROL.2009.09.003.

Kapaj, S., Peterson, H., Liber, K., Bhattacharya, P., 2006. Human health effects from chronic arsenic poisoning - a review. J Environ Sci Health A Tox Hazard Subst Environ Eng 41. https://doi.org/10.1080/10934520600873571.

Kersten, M., Vlasova, N., 2009. Silicate adsorption by goethite at elevated temperatures. Chem. Geol. 262 https://doi.org/10.1016/j.chemgeo.2009.02.002.

Kim, M.J., Nriagu, J., Haack, S., 2000. Carbonate ions and arsenic dissolution by groundwater. Environ. Sci. Technol. 34 https://doi.org/10.1021/es990949p.

Konert, M., Vandenberghe, J., 1997. Comparison of laser grian size analysis with pipette and sieve analysis: a solution for the underestimation of the clay fraction. Sedimentology 44, 523–535.

Langner, P., Mikutta, C., Kretzschmar, R., 2012. Arsenic sequestration by organic sulphur in peat. Nat. Geosci. 5 https://doi.org/10.1038/ngeo1329.

Lin, J.B., Yuan, S., Wang, W., Hu, Z.H., Yu, H.Q., 2016. Precipitation of organic arsenic compounds and their degradation products during struvite formation. J. Hazard Mater. 317 https://doi.org/10.1016/j.jhazmat.2016.05.057.

Lüders, K., Dahmke, A., Fiedler, M., Köber, R., 2020. Temperature influence on mobilisation and (re)fixation of trace elements and heavy metals in column tests with aquifer sediments from 10 to 70 °C. Water Res. 169, 115266 https://doi.org/10.1016/J.WATRES.2019.115266.

Malik, A., Parvaiz, A., Mushtaq, N., Hussain, I., Javed, T., Rehman, H.U., Farooqi, A., 2020. Characterization and role of derived dissolved organic matter on arsenic mobilization in alluvial aquifers of Punjab, Pakistan. Chemosphere 251. https://doi.org/10.1016/j.chemosphere.2020.126374.

Manning, B.A., Goldberg, S., 1996. Modeling competitive adsorption of arsenate with phosphate and molybdate on oxide minerals. Soil Sci. Soc. Am. J. 60 https://doi.org/10.2136/sssaj1996.03615995006000010020x.

Mattheß, G., 1994. Die Beschaffenheit des Grundwassers. Schweizerbart Science Publishers, Stuttgart, Germany.

Morales-Simfors, N., Bundschuh, J., 2022. Arsenic-rich geothermal fluids as environmentally hazardous materials – a global assessment. Sci. Total Environ. 817, 152669 https://doi.org/10.1016/J.SCITOTENV.2021.152669.

Mostert, E., 2020. Water and national identity in The Netherlands; the history of an idea. Water Hist 12. https://doi.org/10.1007/s12685-020-00263-3.

Ngantcha-Kwimi, T.A., Reed, B.E., 2020. Competitive adsorption of as(III), as(V), and PO4 by an iron oxide impregnated activated carbon: surface complex modeling. Water Air Soil Pollut. 231 https://doi.org/10.1007/s11270-020-04853-y.

Nguyen, V.L., Chen, W.H., Young, T., Darby, J., 2011. Effect of interferences on the breakthrough of arsenic: rapid small scale column tests. Water Res. 45, 4069–4080. https://doi.org/10.1016/J.WATRES.2011.04.037.

Nickson, R., McArthur, J., Burgess, W., Matin Ahmed, K., Ravenscroft, P., Rahman, M., 1998. Arsenic poisoning of Bangladesh groundwater [7]. Nature. https://doi.org/10.1038/26387.

Ortega-Guerrero, A., 2017. Evaporative concentration of arsenic in groundwater: health and environmental implications, La Laguna Region, Mexico. Environ. Geochem. Health 39. https://doi.org/10.1007/s10653-016-9866-5.

Paktunc, D., 2013. Mobilization of arsenic from mine tailings through reductive dissolution of goethite influenced by organic cover. Appl. Geochem. 36, 49–56. https://doi.org/10.1016/J.APGEOCHEM.2013.05.012.

Parkhurst, D.L., Appelo, C.A.J., 1999. User's Guide to PHREEQC (Version 2)—A Computer Program for Speciation. Batch-Reaction, One-Dimensional Transport, and Inverse Geochemical Calculations, Washington DC.

Pedersen, H.D., Postma, D., Jakobsen, R., 2006. Release of arsenic associated with the reduction and transformation of iron oxides. Geochem. Cosmochim. Acta 70, 4116–4129. https://doi.org/10.1016/J.GCA.2006.06.1370.

Postma, D., Larsen, F., Minh Hue, N.T., Duc, M.T., Viet, P.H., Nhan, P.Q., Jessen, S., 2007. Arsenic in groundwater of the Red River floodplain, Vietnam: controlling geochemical processes and reactive transport modeling. Geochem. Cosmochim. Acta 71. https://doi.org/10.1016/j.gca.2007.08.020.

Price, R.E., Pichler, T., 2006. Abundance and mineralogical association of arsenic in the Suwannee Limestone (Florida): implications for arsenic release during water–rock interaction. Chem. Geol. 228, 44–56. https://doi.org/10.1016/J.CHEMGEO.2005.11.018.

Rabenhorst, M.C., 1988. Determination of organic and carbonate carbon in calcareous soils using dry combustion. Soil Sci. Soc. Am. J. 52, 965–969.

Ravenscroft, Peter, Brammer, H., Richards, K.S., 2009. Arsenic Pollution : a Global Synthesis. Wiley-Blackwell.

Saaltink, M.W., Ayora, C., Stuyfzand, P.J., Timmer, H., 2003. Analysis of a deep well recharge experiment by calibrating a reactive transport model with field data. J. Contam. Hydrol. 65 https://doi.org/10.1016/S0169-7722(02)00236-X.

Smedley, P.L., 2008. 4: sources and distribution of arsenic in groundwater and aquifers. In: Appelo, C.A.J. (Ed.), Arsenic in Groundwater, a World Problem. Netherlands National Committee IAH, Utrecht, pp. 102–125.

Smedley, P.L., Edmunds, W.M., Pelig-Ba, K.B., 1996. Mobility of arsenic in groundwater in the Obuasi gold-mining area of Ghana: some implications for human health. Geological Society 113. https://doi.org/10.1144/GSL.SP.1996.113.01.13.

Smedley, P.L., Kinniburgh, D.G., 2002. A review of the source, behaviour and distribution of arsenic in natural waters. Appl. Geochem. https://doi.org/10.1016/S0883-2927(02)00018-5.

Smedley, P.L., Nicolli, H.B., Macdonald, D.M.J., Barros, A.J., Tullio, J.O., 2002. Hydrogeochemistry of arsenic and other inorganic constituents in groundwaters from La Pampa, Argentina. Appl. Geochem. 17, 259–284. https://doi.org/10.1016/S0883-2927(01)00082-8.

Smolders, A.J.P., Lucassen, E.C.H.E.T., Bobbink, R., Roelofs, J.G.M., Lamers, L.P.M., 2010. How nitrate leaching from agricultural lands provokes phosphate eutrophication in groundwater fed wetlands: the sulphur bridge. Biogeochemistry 98. https://doi.org/10.1007/s10533-009-9387-8.

Spijker, J., 2008. Arseen in Nederlands Grondwater. Oorzaak Van Verhoogde Arseenconcentraties. RIVM Briefrapport 607300009/2008 Bilthoven.

Stolze, L., Zhang, D., Guo, H., Rolle, M., 2019. Model-based interpretation of groundwater arsenic mobility during in situ reductive transformation of ferrihydrite. Environ. Sci. Technol. 53 https://doi.org/10.1021/acs.est.9b00527.

Stuyfzand, P.J., 1993a. Behaviour of major and trace constituents in fresh and salt intrusion waters, in the western Netherlands. I. In: Custodio, E., Galofré, A. (Eds.), Study and Modelling of Saltwater Intrusion into Aquifers, Proc. 12th Salt Water Intrusion Meeting, CIHS. CIMNE Barcelona, pp. 143–160.

Stuyfzand, P.J., 1993b. Hydrochemistry and Hydrology of the Coastal Dune Area of the Western Netherlands. PhD Thesis. Vrije Universiteit Amsterdam, 366pp. http://dare.ubvu.vu.nl/handle/1871/12716.

Stuyfzand, P.J., 1994. Geohydrochemische aspecten van methaan in grondwater in Nederland. H2O 27, 500–510.

Stuyfzand, P.J., 1995. The impact of land reclamation on groundwater quality and future drinking water supply in The Netherlands. Water Sci. Technol. 31 https://doi.org/10.1016/0273-1223(95)00356-R.

Stuyfzand, P.J., Timmer, H., 1999. Deep Well Injection at the Langerak and Nieuwegein Sites in the Netherlands: Chemical Reactions and Their Modeling. Kiwa Water Research Institute. Report SWE 99.006,44pp.

Stuyfzand, P.J., de Lange, W.J., Zindler, A., 2005. Recognition, dating and genesis of fresh and brackish groundwaters in the Hollandsch Diep estuary in the compound Rhine-Meuse delta. In: Araguas, L., Custodio, E., Manzano, M. (Eds.), Groundwater and Saline Intrusion, Selected Papers from the 18th SWIM. Inst. Geol. Y Minero de Espana, Cartagena, pp. 665–678.

Stuyfzand, P.J., Juhàsz-Holterman, M.H.A., de Lange, W.J., 2006. Riverbank filtration in The Netherlands: well fields, clogging and geochemical reactions. In: Hubbs, S.A. (Ed.), Riverbank Filtration Hydrology. Springer Netherlands, Dordrecht, pp. 119–153.

Stuyfzand, P.J., van Rossum, P., Mendizabal, I., 2008. Does arsenic, in groundwaters of the compound Rhine-Meuse-Scheldt-Ems delta, menace drinking water supply in The Netherlands? In: Appelo (Ed.), Arsenic in Groundwater, a World Problem, Netherlands National Committee IAH Publ, vol. 5, pp. 102–125. http://www.igrac.net/dynamics/modules/SFIL0100/view.php?fil_Id=107.

Stuyfzand, P.J., 2015. Trace element patterns in Dutch coastal dunes after 50 years of artificial recharge with Rhine River water. Environmental Earth Sciences 73 (12), 7833–7849. https://doi.org/10.1007/s12665-014-3770-z.

Stuyfzand, P.J., Aggenbach, C.J.S., Lafort, R., 2014. Diagnose en prognose van de arseenconcentratie in het ruwe water van de winning Ouddorp. Kiwa Water Research Institute report KWR 2014.032, 89pp.

Swedlund, P.J., Webster, J.G., 1999. Adsorption and polymerisation of silicic acid on ferrihydrite, and its effect on arsenic adsorption. Water Res. 33 https://doi.org/10.1016/S0043-1354(99)00055-X.

Tchounwou, P.B., Yedjou, C.G., Udensi, U.K., Pacurari, M., Stevens, J.J., Patlolla, A.K., Noubissi, F., Kumar, S., 2019. State of the science review of the health effects of inorganic arsenic: perspectives for future research. Environ. Toxicol. 34 https://doi.org/10.1002/tox.22673.

TNO (not dated), Data en informatie van de Nederlandse Ondergrond. website. https://www.dinoloket.nl/. (Accessed 23 December 2022).

Ullman, W.J., Aller, R.C., 1985. The geochemistry of iodine in near-shore carbonate sediments. Geochem. Cosmochim. Acta 49. https://doi.org/10.1016/0016-7037(85)90311-4.

Van Beek, C., Hettinga, F., Straatman, R., 1989. The Effects of Manure Spreading and Acid Deposition upon Groundwater Quality at Vierlingsbeek. IAHS-AISH publication, the Netherlands.

Van Beek, C., Van der Jagt, H., 1996. Mobilization and speciation of trace elements in groundwater. In: IWSA International Workshop "Natural Origin Inorganic Micropollutants: Arsenic and Other Constituents", Vienna May, pp. 6–7.

Van Beek, C.G.E.M., Boukes, H., Van Rijsbergen, D., Straatman, R., 1988. The threat of The Netherlands water works by nitrate in the abstracted groundwater, as demonstrated on the well field Vierlingsbeek. Water Supply 6.

Van Rossum, P., 1998. Mobilisation and Origin of Arsenic in the Subsoil of the Province of North Holland (In Dutch). Amsterdam.

Leefbaar laagland. Geschiedenis van de waterbeheersing en landaanwinning in Nederland. In: Van de Ven (Ed.), 2003. Matrijs, Utrecht.

Van Rossum, P., 1996. Distribution of Arsenic in Soil and Groundwater of the Province of North Holland (In Dutch). Amsterdam.

Vandenbohede, A., Wallis, I., Alleman, T., 2019. Trace metal behavior during in-situ iron removal tests in Leuven, Belgium. Sci. Total Environ. 648, 367–376. https://doi.org/10.1016/j.scitotenv.2018.08.126.

Vermooten, S., Gunnink, J., 2006. Arsenic in the Dutch coastal provinces. In: Appelo, C.A.J. (Ed.), Arsenic in Groundwater, a World Problem. Netherlands National Committee IAH, Utrecht, pp. 102–125.

Wang, Y., Le Pape, P., Morin, G., Asta, M.P., King, G., Bártová, B., Suvorova, E., Frutschi, M., Ikogou, M., Pham, V.H.C., Vo, P. Le, Herman, F., Charlet, L., Bernier-Latmani, R., 2018. Arsenic speciation in mekong delta sediments depends on their depositional environment. Environ. Sci. Technol. 52 https://doi.org/10.1021/acs.est.7b05177.

Webster, J.G., Nordstrom, D.K., 2003. Chapter 4: geothermal Arsenic. The source, transport and fate of arsenic in geothermal systems, in: arsenic in Ground Water. In: Appelo, C.A.J. (Ed.), Arsenic in Groundwater, a World Problem. Netherlands National Committee IAH, Utrecht, pp. 102–125.

Weil, M., 2008. The struvite-type compounds M[Mg(H2O)6](XO 4), where M = Rb, Tl and X = P, as. Cryst. Res. Technol. 43 https://doi.org/10.1002/crat.200800403.

Welch, A.H., Westjohn, D.B., Helsel, D.R., Wanty, R.B., 2000. Arsenic in ground water of the United States: occurrence and geochemistry. Ground Water 38. https://doi.org/10.1111/j.1745-6584.2000.tb00251.x.

Wesselink, M., Liu, W., Koornneef, J., van den Broek, M., 2018. Conceptual market potential framework of high temperature aquifer thermal energy storage - a case study in The Netherlands. Energy 147. https://doi.org/10.1016/j.energy.2018.01.072.

Williams, M., Fordyce, F., Paijitprapapon, A., Charoenchaisri, P., 1996. Arsenic contamination in surface drainage and groundwater in part of the southeast Asian tin belt, Nakhon Si Thammarat Province, southern Thailand. Environ. Geol. 27, 16–33. https://doi.org/10.1007/BF00770599.

World Health Organization, 2019. Preventing Disease through Healthy Environment. Exposure to Arsenic: A Major Public Health Concern. Preventing Disease through Healthy Environment. WHO REFERENCE NUMBER: WHO/CED/PHE/EPE/19.4.1 Department of Public Health. Environmental and Social Determinants of Health World Health Organization, Geneva, Switzerland.

Wu, K., Zhang, N., Liu, T., Ma, C., Jin, P., Zhang, F., Zhang, J., Wang, X., 2017. Competitive adsorption behaviors of arsenite and fluoride onto manganese-aluminum binary adsorbents. Colloids Surf. A Physicochem. Eng. Asp. 529 https://doi.org/10.1016/j.colsurfa.2017.05.039.

Xing, S., Guo, H., Zhang, L., Wang, Z., Sun, X., 2022. Silicate weathering contributed to arsenic enrichment in geotherm-affected groundwater in Pliocene aquifers of the Guide basin, China. J. Hydrol. (Amst.) 606, 127444. https://doi.org/10.1016/J.JHYDROL.2022.127444.

Xu, H., Allard, B., Grimvall, A., 1988. Influence of pH and organic substance on the adsorption of As(V) on geologic materials. Water Air Soil Pollut. 40 https://doi.org/10.1007/BF00163734.

Zhang, Y.C., Slomp, C.P., Broers, H.P., Bostick, B., Passier, H.F., Böttcher, M.E., Omoregie, E.O., Lloyd, J.R., Polya, D.A., Van Cappellen, P., 2012. Isotopic and microbiological signatures of pyrite-driven denitrification in a sandy aquifer. Chem. Geol. 300–301. https://doi.org/10.1016/j.chemgeo.2012.01.024.

Zhang, Y.C., Slomp, C.P., Broers, H.P., Passier, H.F., Cappellen, P. Van, 2009. Denitrification coupled to pyrite oxidation and changes in groundwater quality in a shallow sandy aquifer. Geochem. Cosmochim. Acta 73, 6716–6726. https://doi.org/10.1016/J.GCA.2009.08.026.